GLOBAL CLIMATE BULLETIN
n°201 – March 2016

Table of Contents

I. DESCRIPTION OF THE CLIMATE SYSTEM (JANUARY 2016)

I.1.OCEANIC ANALYSIS

I.1.a Global analysis

In the Pacific ocean :

- Along the equatorial waveguide : (fig.I.1.1, I.1.2 and I.1.3): The presence of the El Nino phenomenon is still visible on the map of SST anomalies.. Strong warm anomalies along the equator from the International Date Line to the South American coasts are still very strong. The SST anomaly hasn't changed much between December and January in the basin center between 120W and 160W (see fig. I.1.1 bottom), with a light decrease of the Nino3.4 index from 2.9°C to 2.8°C Nevertheless, the trend is a decline of both sides, with in the west a decrease of 0.3 ° C of Nino4 index and in the east, between 120W and the South American coast an even stronger fall (-0.8 ° C of Nino1+2 index).

Nino indices thus achieved comparable strong surface values at year-end 2015, comparable to the 1997/1998 event record; however subsurface temperature anomalies remained substantially weaker (Fig I. 1c). The warm anomaly in the eastern basin has clearly decreased in January, while the cold anomaly in the west was strengthened.

So the phenomenon peaked in December and initiated an early decline in January. To monitor in February : a Kelvin wave, visible at the end of Hovmuller diagram (Figure I.1.b), which could temporarily slow the decline in eastern basin.
In the northern hemisphere: still a clear positive structure of the PDO with a 0.8 index value, despite a cooling trend in the east of Northern Pacific.
In the southern hemisphere: the horseshoe structure, quite symmetrical in the northern hemisphere, was strengthened with an accentuation of the central cold anomaly and of the hot anomaly around to North-east, East and South-east.

On the Continent Maritime:
SST still warming in January in connection with the activity of the MJO (fig I.2.b)

In the Indian Ocean :

Widespread warm anomaly persists, but with a downward trend at the neighborhood of Africa and an upward trend near the Maritime Continent. Hence a negative DMI index in January (-0.65 ° C). see http://stateoftheocean.osmc.noaa.gov/sur/ind/dmi.php)

In the Atlantic:
Continued strong cold anomaly in the center of the North Atlantic. Between 30 ° N and 30 ° S, the Atlantic is generally warmer than normal. As in the Pacific there is some structural symmetry with a cold anomaly well marked in the center and west of the South Atlantic.

In the Mediterraen :
Persistent generalized warm anomaly.

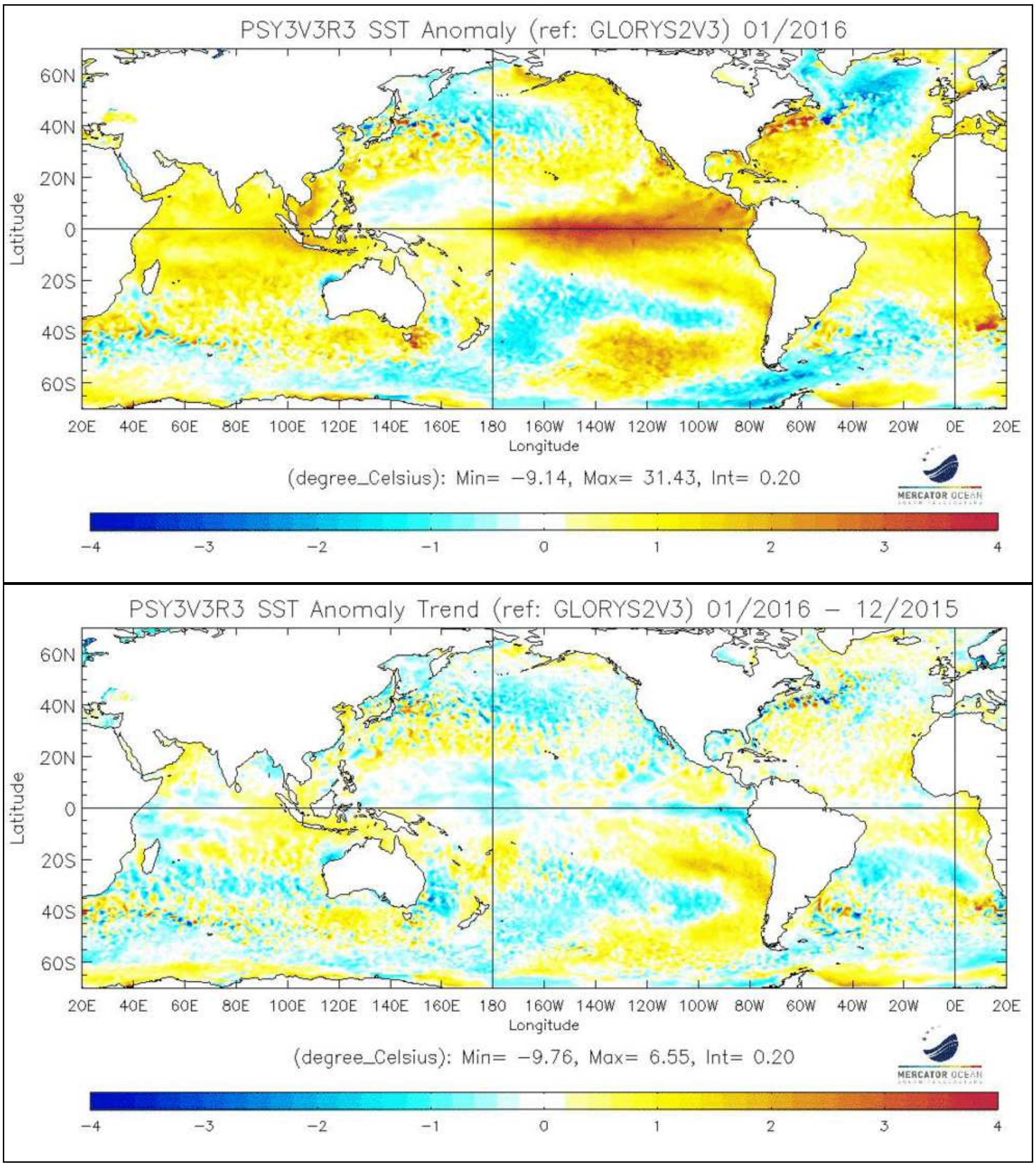

fig.I.1.1: top : SSTs Anomalies (°C) . Bottom : SST tendency (current – previous month), (reference Glorys 1992-2009). http://bcg.mercator-ocean.fr/

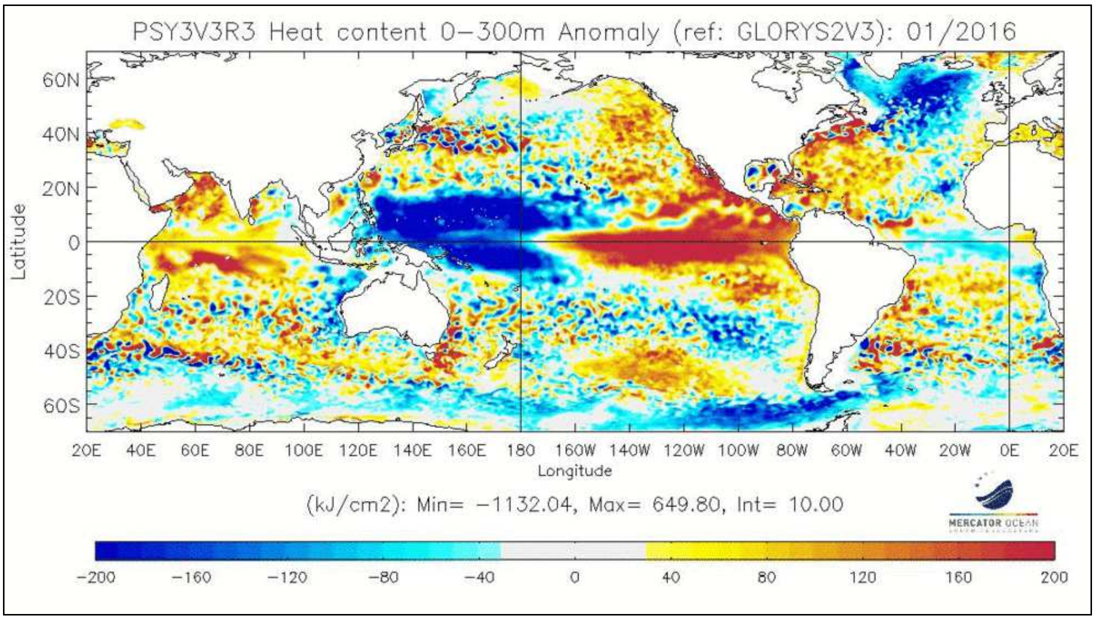

fig.I.1.2: map of Heat Content Anomalies (first 300m, kJ/cm2, reference Glorys 1992-2009)

http://bcg.mercator-ocean.fr/

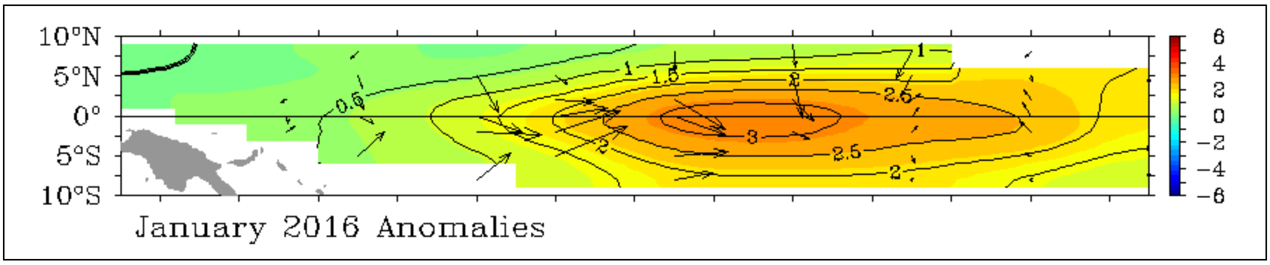

fig.I.1.3: SST Anomalies and Wind anomalies over the Equatorial Pacific from TAO/TRITON.

http://www.pmel.noaa.gov/tao/jsdisplay/monthly-summary/monthly-summary.html

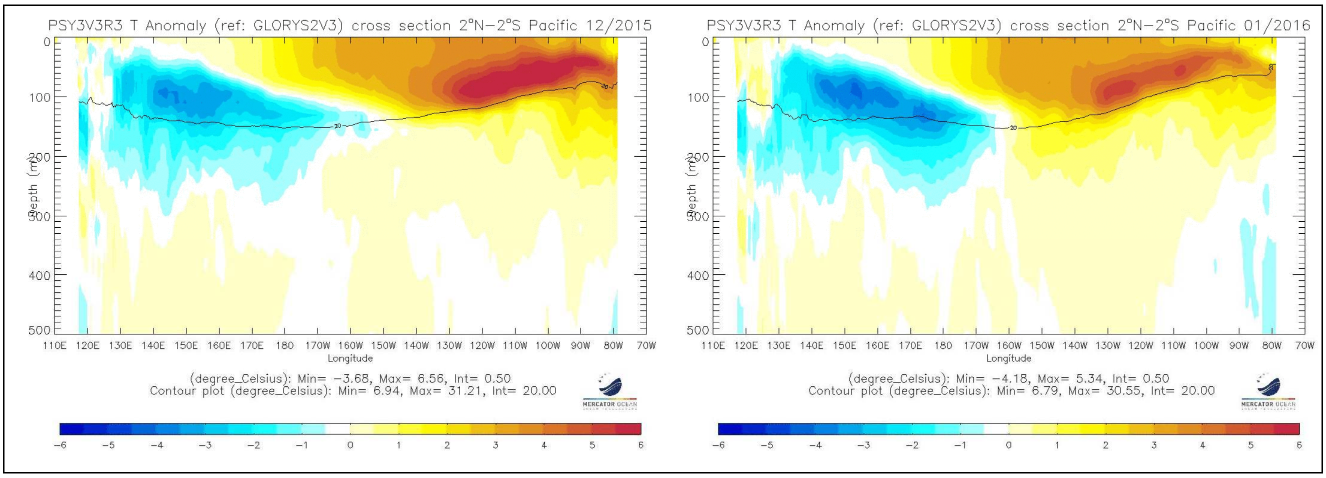

fig.I.1.4: Oceanic temperature anomaly in the first 500 meters in the Equatorial Pacific (previous and current month), http://bcg.mercator-ocean.fr

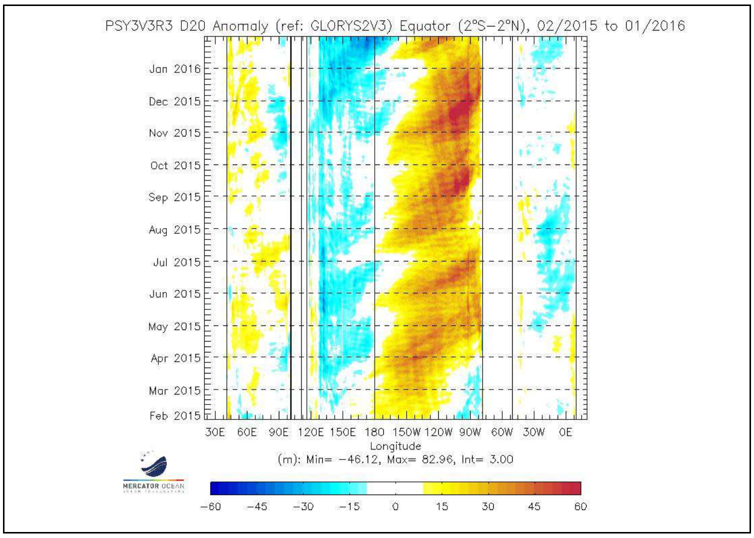

fig.I.1.5: Hovmüller diagram of Thermocline Depth Anomalies (m) (depth of the 20°C isotherm) along the equator for all oceanic basins over a 6 month period http://bcg.mercator-ocean.fr/

I.1.b Near Europe

Generally quite little change of SST anomalies and their patterns near Europe from December 2015 to January 2016. Almost all sea surfaces near Europe were still warmer than normal. To be noted the ongoing warming in the Arctic region, especially around Svalbard, which is normally frozen in January. The Baltic Sea was influenced by some cold air outbreaks, so the northern parts of the Baltic Sea surfaces were frozen and there were partly colder-than-normal anomalies near the coasts. In contrast, the North Sea surfaces profited from warm air advection.

The large cold anomaly over the central North Atlantic remained quasi unchanged in position and extension, and there were no major changes in intensity either.

Also still warm with high persistency at the Biscay and in the Mediterranean. Anomalies in the Eastern Mediterranean decreased slightly but were still above normal.

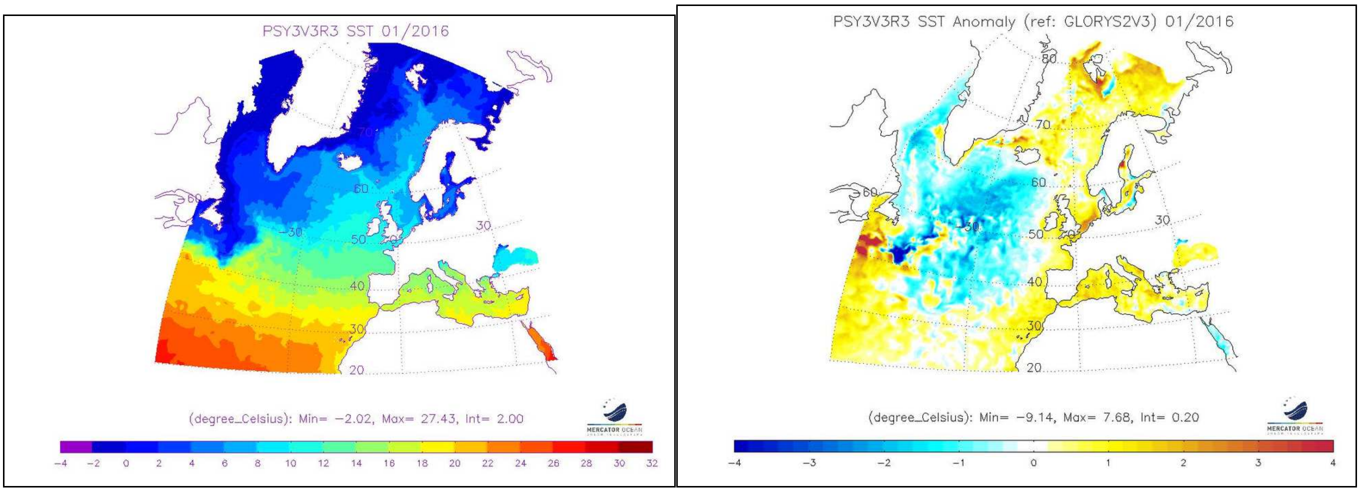

fig.I.1.6 : Mean sea surface temperature in the RA VI Region (Europe) and anomaly (reference Glorys 1992-2009). http://bcg.mercator-ocean.fr/

I.2.ATMOSPHÈRE

I.2.a General Circulation

Strong Ocean-Atmosphere coupling.

Velocity Potential Anomaly field in the high troposphere (fig. 1.2.1 – insight into Hadley-Walker circulation anomalies) :
The main dipole on the Pacific is well correlated with SST anomalies with a strong core of upward motion on the center of the basin, and a very strong subsidence in the Maritime Continent. The MJO on the first 2 decades of January has probably reinforced the negative anomaly on the Maritime Continent. Still a quite strong upward motion core near South America centered in January over the Atlantic, northward of the Guyana. An extension of the main upward motion area stretches to the Gulf of Mexico and southern United States. A weaker subsidence area covers Africa and western half of the Indian Ocean.
Strong negative SOI index in January : -2.2.

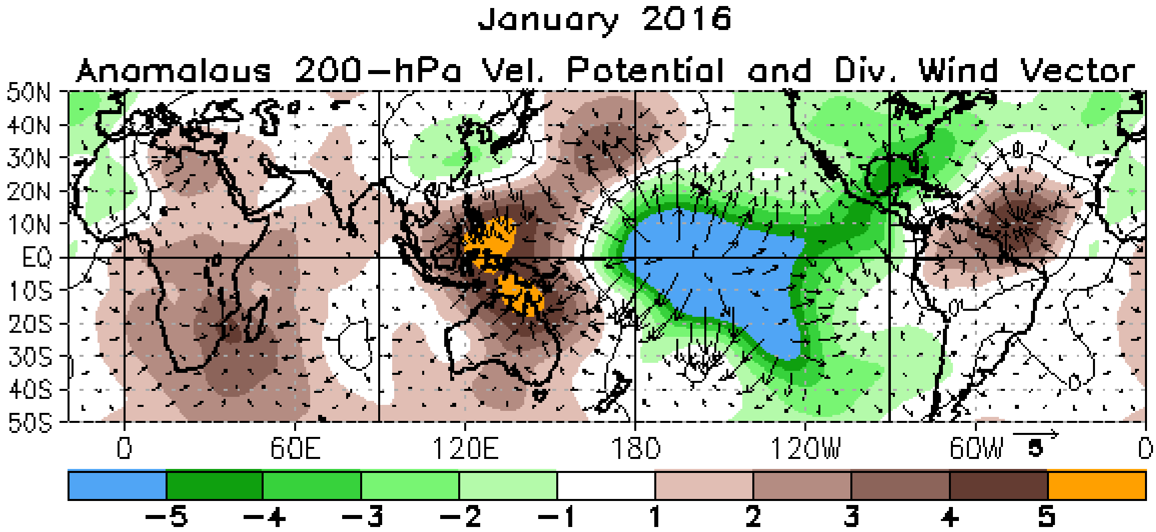

fig.I.2.1: Velocity Potential Anomalies at 200 hPa and associated divergent circulation anomaly. Green (brown) indicates a divergence-upward anomaly (convergence-downward anomaly).
http://www.cpc.ncep.noaa.gov/products/CDB/Tropics/figt24.shtml

MJO (fig. I.2.b):

MJO was active in quarter 7,8,1,2 during the 2 first decades.

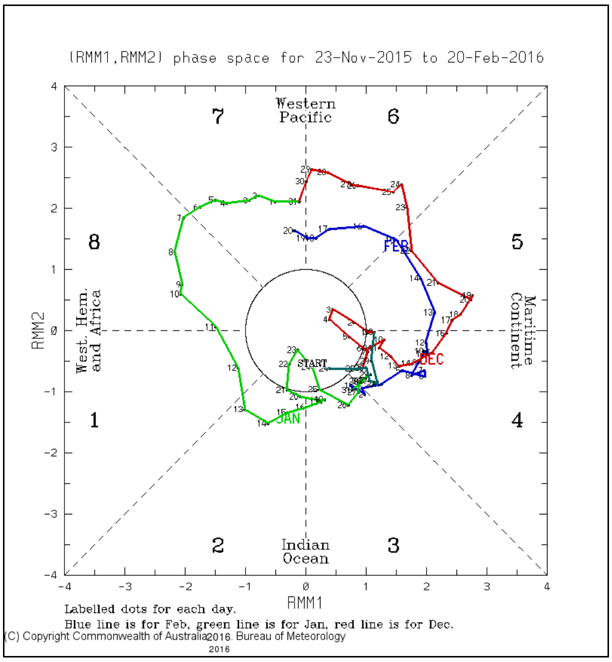

fig.I.2.b: indices MJO http://cawcr.gov.au/staff/mwheeler/maproom/RMM/phase.Last90days.gif

Stream Function anomalies in the high troposphere (fig. 1.2.2 – insight into teleconnection patterns tropically forced) :

The January stream function structures can not be classically related to abnormalities velocity potential. No teleconnection towards the middle latitudes are visible.

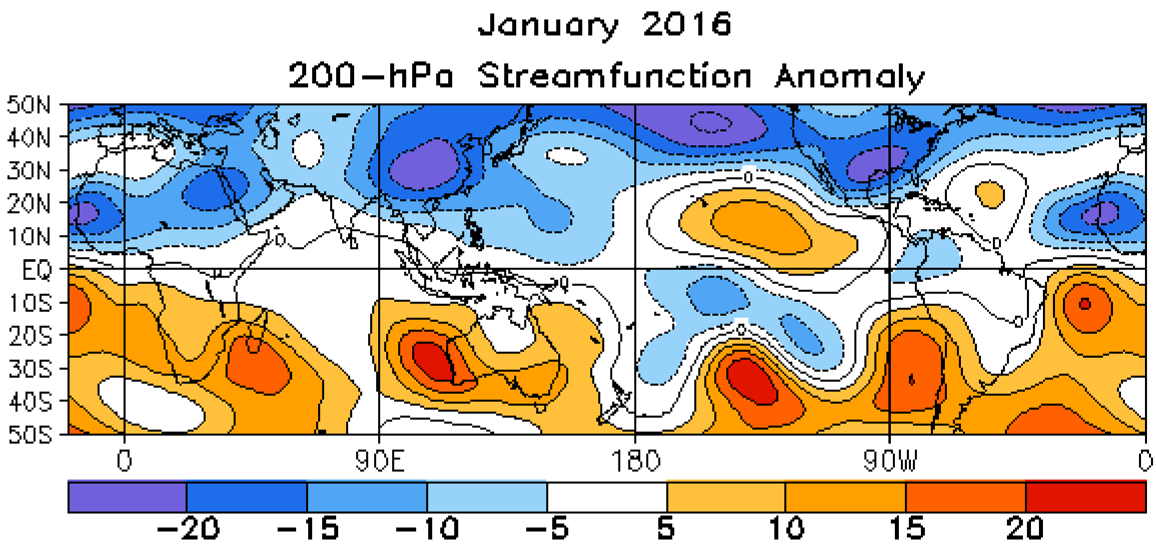

fig.I.2.2: Stream Function Anomalies at 200 hPa.

http://www.cpc.ncep.noaa.gov/products/CDB/Tropics/figt22.shtml

Geopotential height at 500 hPa (fig. 8 – insight into mid-latitude general circulation) :

Despite the lack of high troposphere teleconnection, PNA structure is quite marked in January (index value : +2), giving an area of low géopotentiel the North Pacific, high values on Canada and low values on the south the United States.

On the Atlantic, the low values in southern Iceland were extended on the north and center of Europe. While high geopotential area centered on the Maghreb has protected the Mediterranean.

Very strong positive anomaly on the Siberia.

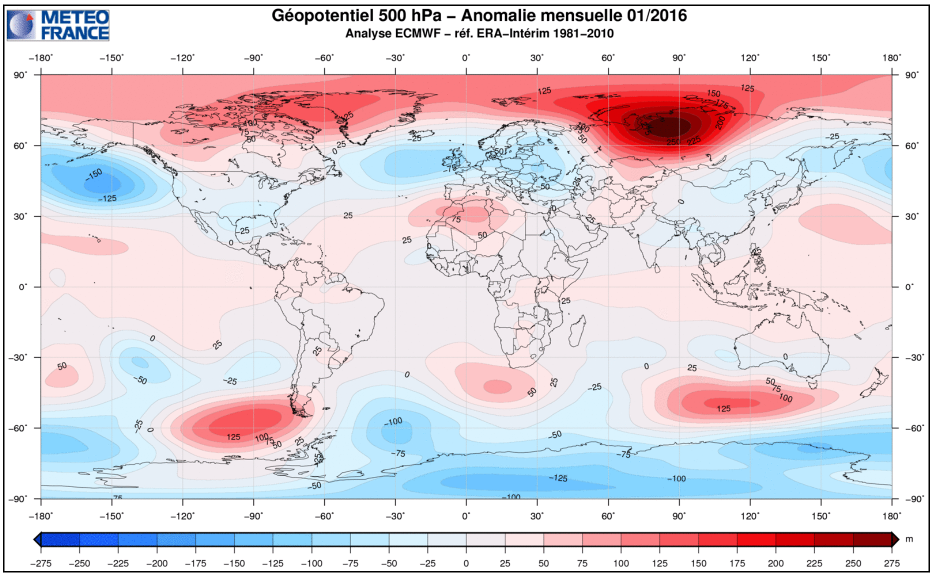

fig.I.2.3: Anomalies of Geopotential height at 500hPa (Meteo-France)

MONTH	NAO	EA	WP	EP-NP	PNA	TNH	EATL/WRUS	SCAND	POLEUR
JAN 16	**-0.4**	**1.0**	**1.0**	**-0.4**	**1.9**	**-0.3**	**-0.5**	**-0.7**	**-2.6**
DEC 15	2.0	3.1	0.6	---	0.5	0.0	1.3	0.1	0.6
NOV 15	1.7	1.6	0.8	-0.9	-0.2	---	0.6	-0.4	-0.7
OCT 15	1.0	0.2	-0.8	0.3	2.1	---	0.6	0.6	-0.5
SEP 15	-0.5	0.2	-1.4	-1.4	-0.8	---	-1.7	1.1	-0.1
AUG 15	-1.1	1.1	-1.5	-0.3	0.1	---	-0.4	0.9	0.1
JUL 15	-3.1	0.2	0.8	0.2	0.3	---	2.0	-1.1	0.4
JUN 15	0.2	1.1	-0.0	1.7	-0.1	---	-0.8	-1.5	-0.2
MAY 15	0.2	0.7	2.1	0.5	-0.1	---	-1.5	-2.1	0.5

Evolution of the main atmospheric indices for the Northern Hemisphere for the last 6 months :

http://www.cpc.ncep.noaa.gov/products/CDB/Extratropics/table3.shtml

Sea level pressure and circulation types over Europe

A remarkable feature this month was a strong deformation of the polar vortex resulting in a very meandering circulation pattern particularly over Europe. It is visible through high positive 500 hPa geopotential anomalies over Greenland/Canada and especially over Russia, whereas most of Europe had negative anomalies. Geopotential was also generally higher than normal around the North Pole, influenced by a very strong negative POLEUR pattern.

Furthermore, an EA pattern still existed but weakened from December to January (index decreased from +3.1 to +1.0). This can also be seen through weakening of both the Icelandic Low and the subtropical European High and their anomalies in both the middle atmosphere and near surface. While southern Europe still had much high pressure influence, northern and middle latitudes in Europe were frequently affected by intense Atlantic cyclonic patterns, particularly northwestern Europe. A slightly negative SCAND pattern (index = -0.7) also contributed to cyclonic influence in northern Europe.

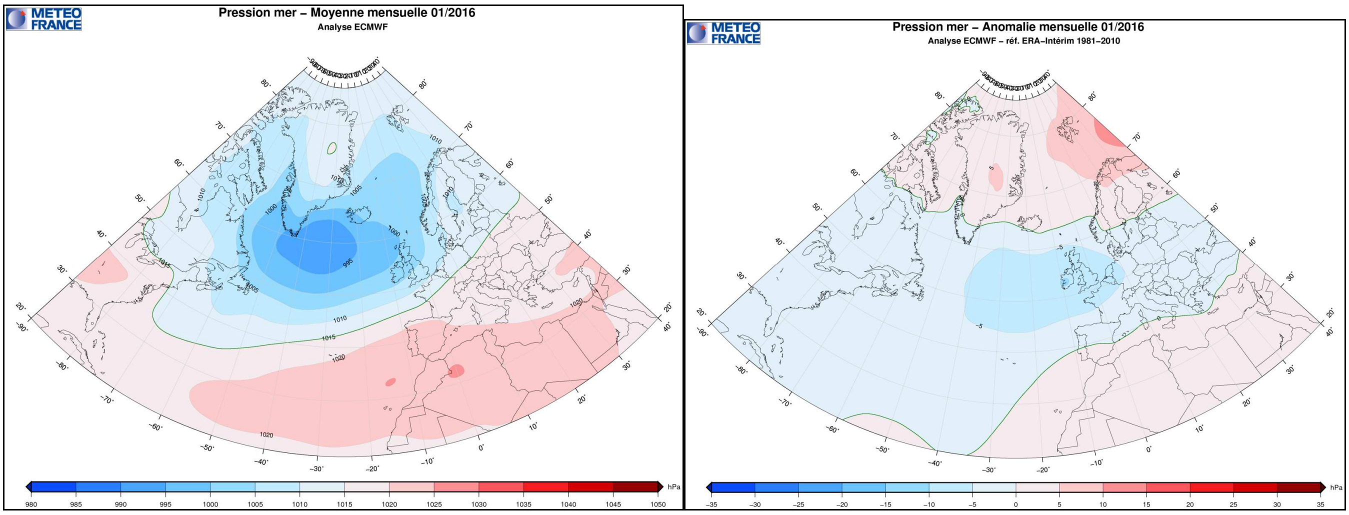

fig.I.2.4: Mean sea level pressure in the RA VI Region (Europe) (top) and 1981-2010 anomalies (bottom).

Circulation indices: NAO and AO

After a positive phase in December, NAO turned to a longer negative phase during January, which ended at the end of the month. The same, but even more extreme can be seen for AO. This reflects the switch to a more meridional structure with increasing air mass exchange between polar and middle latitudes over the northern hemisphere and hence a deformation and a general weakening of the polar vortex.

According to some literature studies, a strong positive NAO in November/December and a weakening afterwards in January is quite typical for El Niño (see e.g. Moron, V., and G. Plaut (2003): The impact of El Niño-southern oscillation upon weather regimes over Europe and the North Atlantic during boreal winter, International Journal of Climatology 23, 363-379)

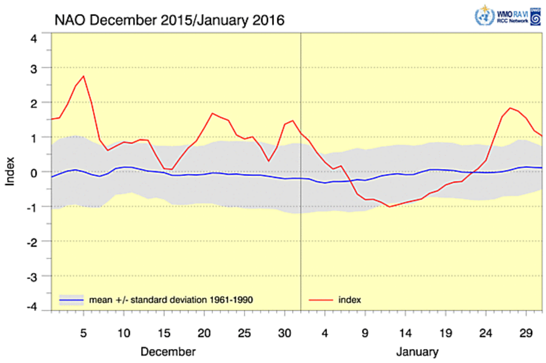

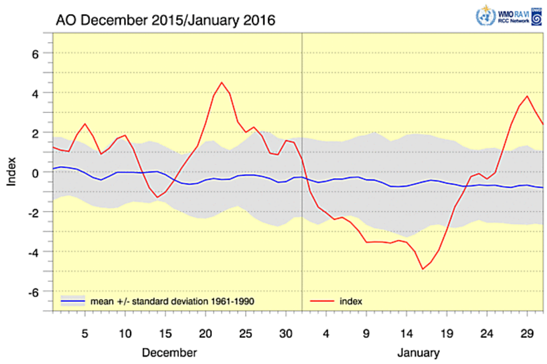

fig.I.2.5: North Atlantic Oscillation (NAO, left) and Arctic Oscillation (AO, right) indices with 1961-1990 mean standard deviation (shading). http://www.dwd.de/rcc-cm , data from NOAA CPC: http://www.cpc.ncep.noaa.gov/products/precip/CWlink/daily_ao_index/teleconnections.shtml

I.2.b Precipitation

In line with the SST and velocity potential field, wide dry zone on the Maritime Continent extending to southern Polynesia. Area of strong positive rainfall anomaly in the central equatorial Pacific.

Persistence in January of a drier than normal area over northern South America but less extended than in previous months, while the Northeast of Brazil have regained normal rainfall.

On Europe (Figure 1.2.5) : more rain than normal in general except for Scandinavia on the one hand and the regions bordering the western Mediterranean on the other.

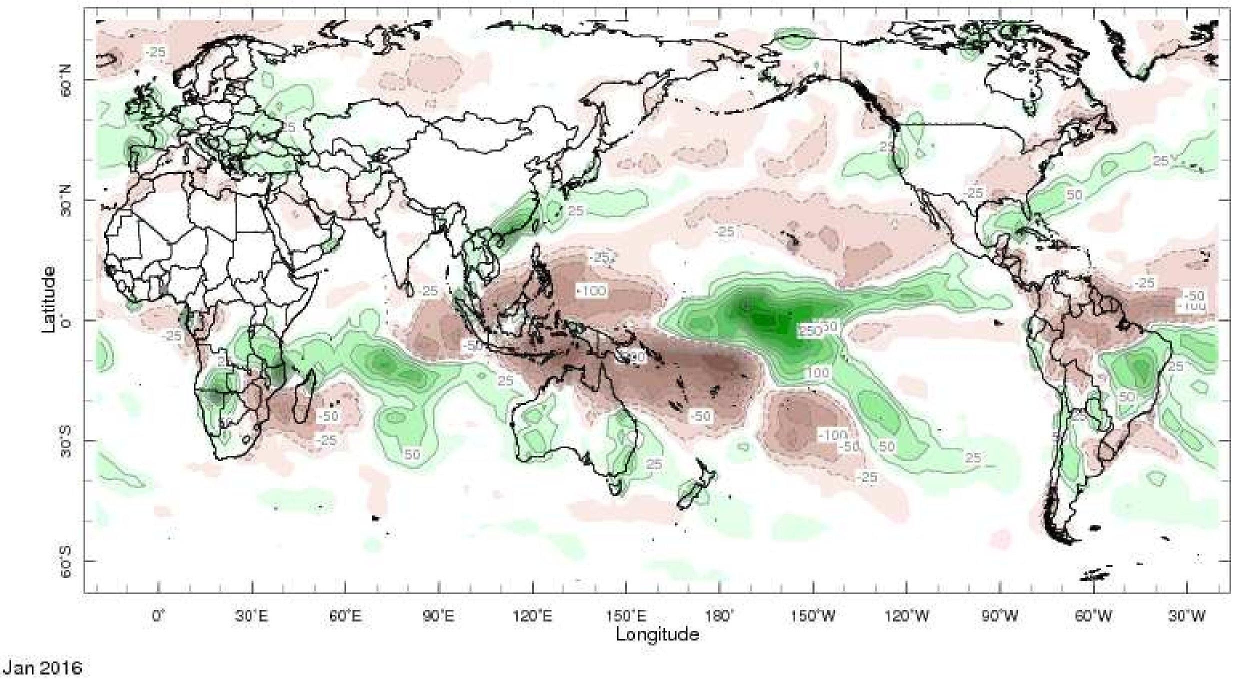

fig.I.2.4: Rainfall Anomalies (mm) (departure to the 1979-2000 normal) – Green corresponds to above normal rainfall while brown indicates below normal rainfall.

http://iridl.ldeo.columbia.edu/maproom/.Global/.Precipitation/Anomaly.html

Precipitation anomalies in Europe:

It was wet especially in middle latitudes from western to eastern Europe, in line with Atlantic cyclonic influence triggered by the EA pattern. Frequent troughs over eastern Europe caused relatively much precipitation in the whole area there.

There was below-normal precipitation at the west coast of Norway because the Atlantic airflow mostly occurred further southwards over the middle latitudes.

Occasionally cyclonic influence also reached southern Europe with some intense rain, but there were also some dry regions, e.g. southern Spain, southeastern France, northern Italy due to some high pressure influence of the subtropical high.

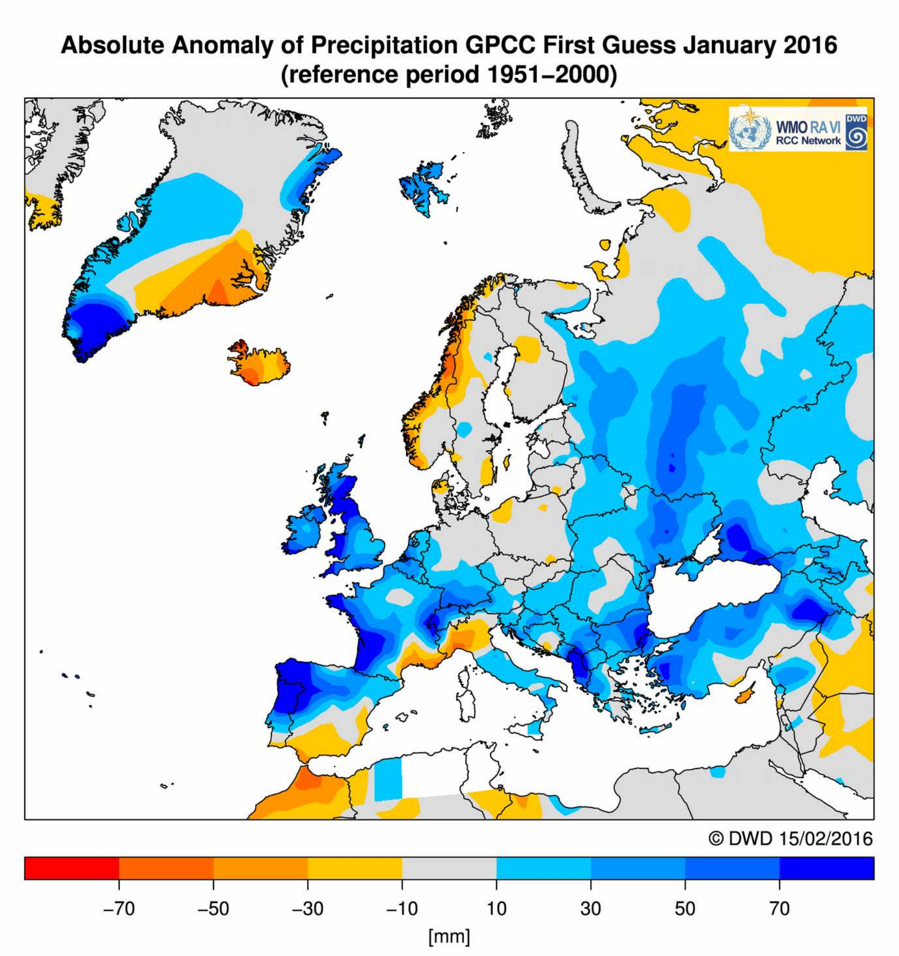

fig.I.2.5: Left: Absolute anomaly (1951-2000 reference) of precipitation in the RA VI Region (Europe), data from GPCC (Global Precipitation Climatology Centre), http://www.dwd.de/rcc-cm. Right: Percentiles of precipitation, 1981-2010 reference. Data from NOAA Climate Prediction Center, http://iridl.ldeo.columbia.edu/maproom/Global/Precipitation/Percentiles.html

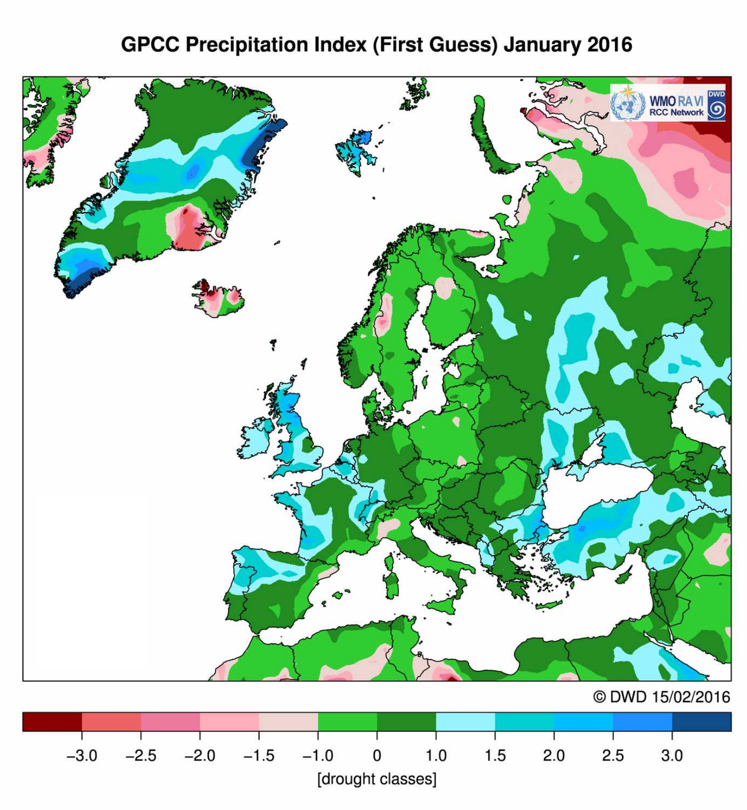

fig. I.2.5a: GPCP Precipitation Index http://www.dwd.de/rcc-cm .

Monthly mean precipitation anomalies in European subregions. Subregions refer to ECMWF land boxes defined in Annex III.3. Anomalies are based on gridded data from GPCC First Guess Product, ftp://ftp-anon.dwd.de/pub/data/gpcc/PDF/GPCC_intro_products_2008.pdf, 1951-2000 reference.

Subregion	**Absolute anomaly**	**GPCP Drought Index**
Northern Europe	+9.8 mm	Not available
Southern Europe	+12.1 mm	Not available

Please note: new drought index since January 2016. The GPCC drought index, which also considers evaporation in addition to precipitation replaces the former SPI-DWD.

Box data for this new index are not available at the moment, but will be provided in future.

I.2.c Temperature

Strong positive anomaly on the high latitude regions of the Northern Hemisphere: Alaska, Canada, Greenland, northern Siberia. cold anomaly in Scandinavia, Russia and southern Siberia, Mongolia and China. warm anomaly on western Europe and West Africa. warm anomaly on the extreme north of South America, Equatorial Africa and the Middle East.

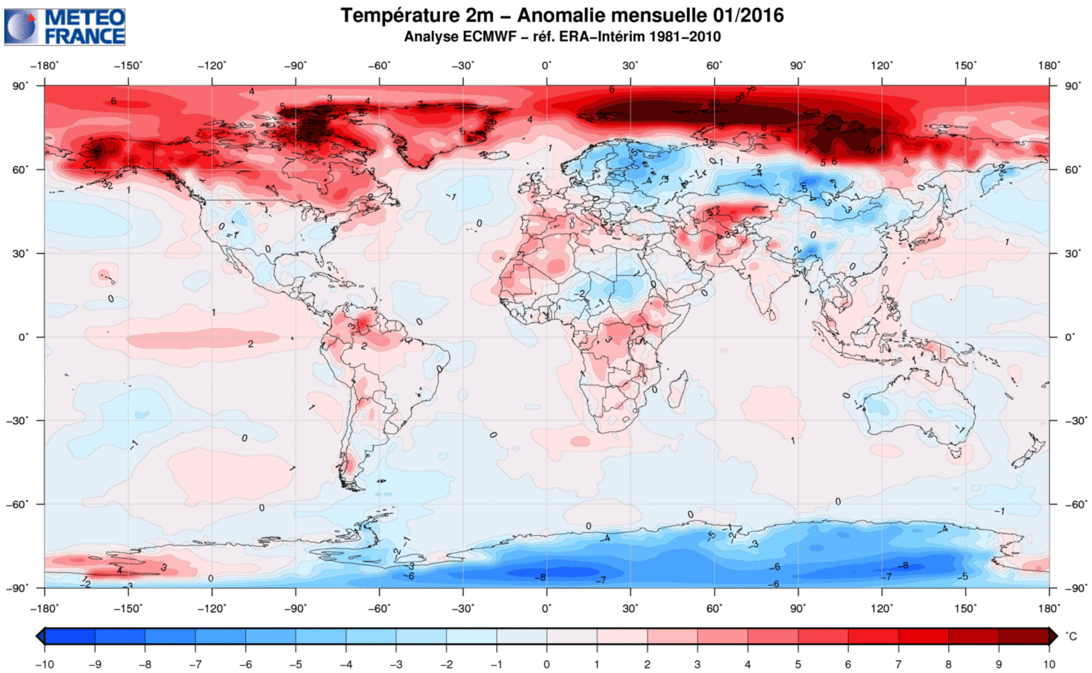

fig.I.2.8: Temperature Anomalies (°C) (Meteo-France)

<u>Temperature anomalies in Europe:</u>

Mainly positive anomalies over Europe in the west and south, negative anomalies in the north and east. Warming in western Europe mainly comes from mild Atlantic air advection, while in the southwest there should have also been a contribution from high pressure subsidence. In northeastern Europe, cold Arctic air outbreaks advanced to the south, mainly in the middle and upper atmosphere.

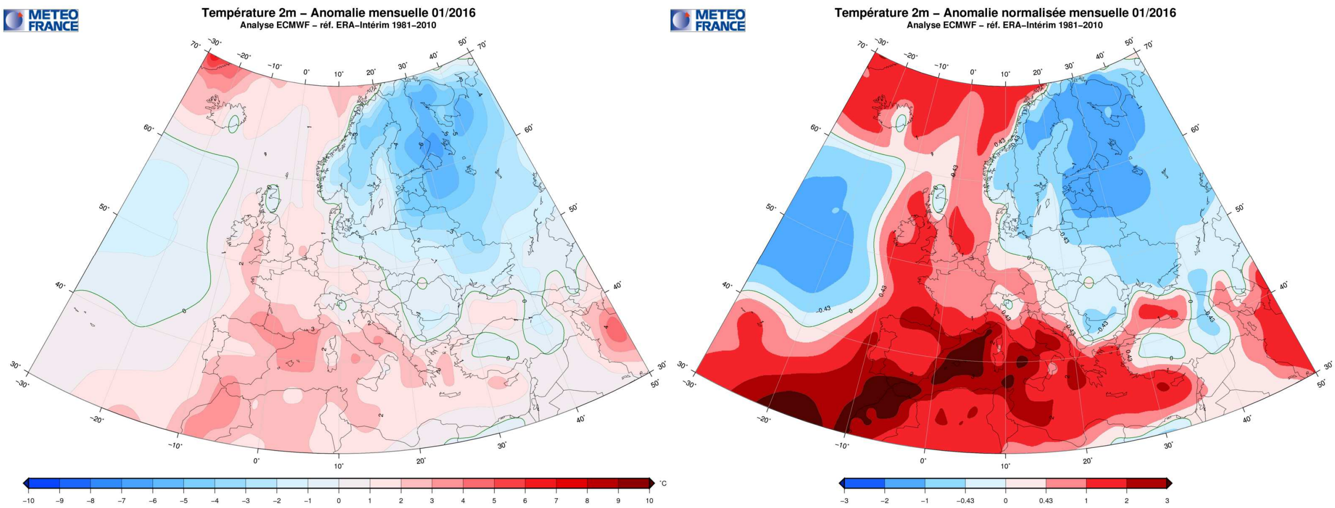

fig.I.2.9: Left graph: Absolute anomaly of temperature in the RA VI Region (Europe). Right graph: Standardized temperature anomalies

Monthly mean temperature anomalies in European subregions: Subregions refer to ECMWF land boxes defined in Annex III.3. Anomalies are based on gridded CLIMAT data from DWD, http://www.dwd.de/rcc-cm, 1961-1990 reference.

Subregion	Anomaly
Northern Europe	+4.1°C
Southern Europe	+2.0°C

I.2.d Sea ice

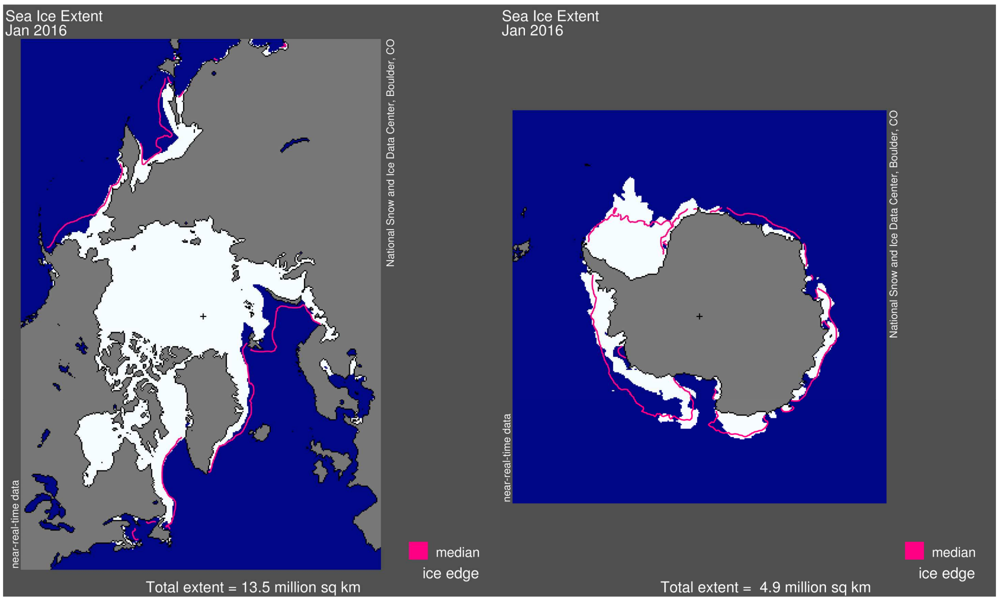

fig.I.2.15: Sea-Ice extension in Arctic (left), and in Antarctic (right). The pink line indicates the averaged extension (for the 1979-2000 period). http://nsidc.org/data/seaice_index/

In Arctic (fig. 1.2.15 and 1.2.16 - left): persistent significant deficit (~ -2 std).

In Antarctic (fig. 1.2.15 and 1.2.16 - right): near normal values.

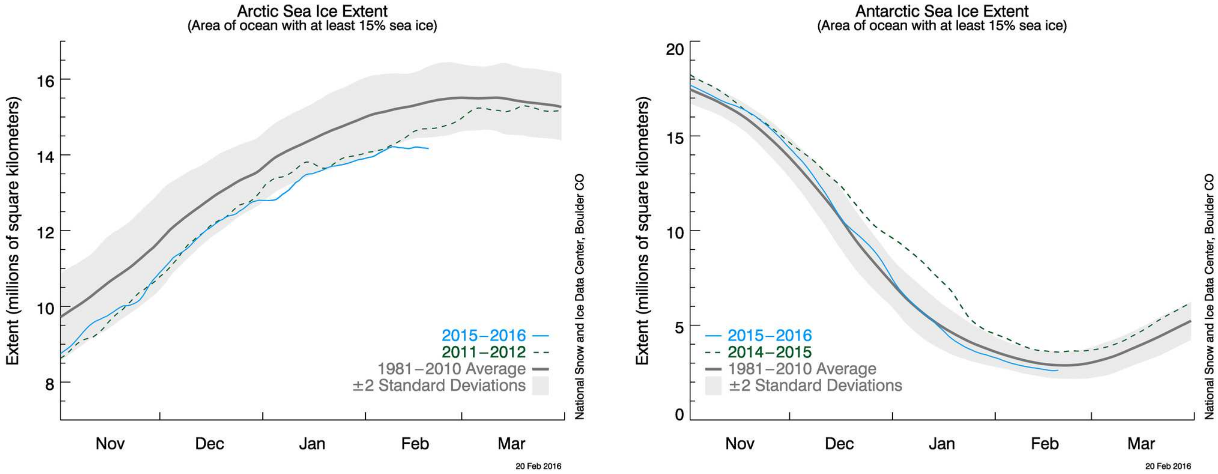

fig. I.2.16 : Sea-Ice extension evolution from NSIDC.

http://nsidc.org/data/seaice_index/images/daily_images/N_stddev_timeseries.png

II. SEASONAL FORECAST FROM DYNAMICAL MODELS

II.1. OCEANIC FORECASTS

The current El Nino event, even in its decreasing phase, continues to strongly constrain the global climate system, thus enhancing its stability and predictability. All seasonal forecast models offer very similar simulations in the Pacific and in tropical areas with consistent and stable structures of a forecast to the next, both in the ocean and for the atmosphere.

II.1.a Sea surface temperature (SST)

Good stability in the El Nino context.

Pacific Ocean: surface warm anomaly in the central and eastern equatorial rail (El Niño) is expected to lose some of its intensity but extend geographically in the east of the basin to the coasts of America South. The PDO positive structure could strengthen during the next 3 months with a greater contrast between the unusually cold water in central North Pacific and the warm waters at its eastern periphery.
In the southern hemisphere, the cold anomaly appears to decline slightly with the spread of warm waters in the east.

Indian Ocean: Remaining of the generalized warm anomaly.

Atlantic Ocean : As in previous months, the tropical Atlantic is the only area where models diverge significantly with a very clear difference between ECMWF and ARP on one hand (warm anomalies), and NCEP on the other hand (significant cold anomaly) . The EUROSIP average is neutral but unreliable in this area. The models agree on the persistence of the strong cold anomaly on the North Atlantic and of warm anomaly from Caribbean and Canadian coasts to Africa, with a strong positive anomaly near Canada.

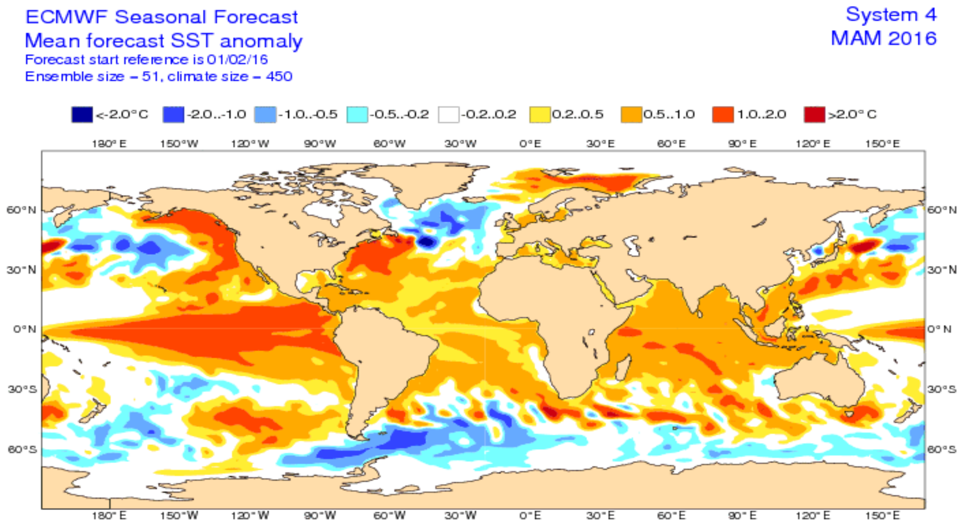

fig.II.1.1: SST anomaly forecast from ECMWF

http://www.ecmwf.int/products/forecasts/d/charts/seasonal/forecast/seasonal_range_forecast/group/

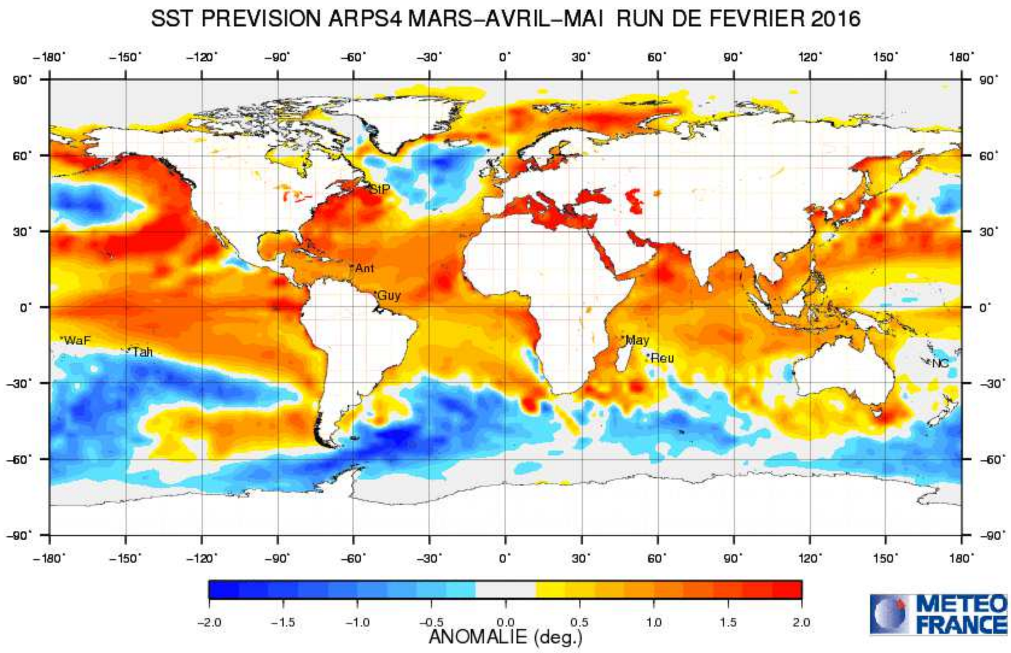

fig.II.1.2: SST Anomaly forecast from Meteo-France (recalibrated with respect of observation).

http://elaboration.seasonal.meteo.fr

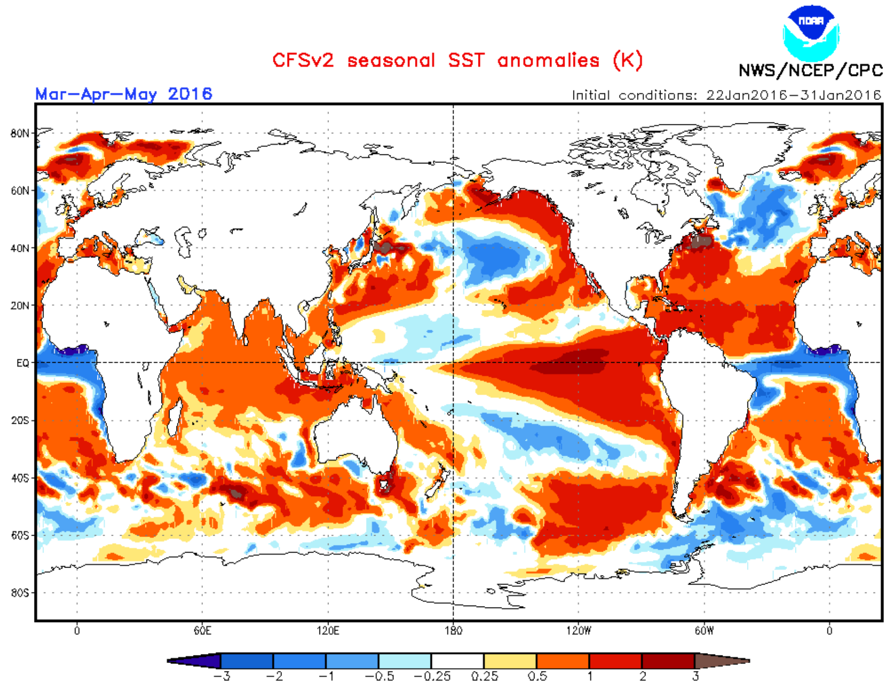

fig.II.1.3: SST anomaly forecast from NCEP.

http://www.cpc.ncep.noaa.gov/products/people/wwang/cfsv2fcst/imagesInd1/glbSSTSeaInd1.gif

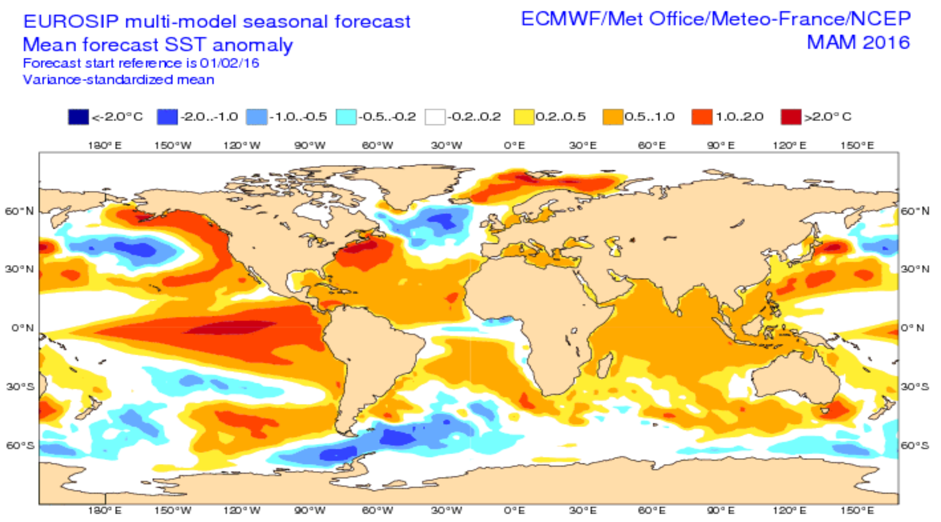

fig.II.1.4: SST Forecasted anomaly from Euro-SIP

II.1.b ENSO forecast

Forecast Phase: fast decreasing of El Niño

The models are very close and very consistent in the forecast of El Nino event evolution. The anomaly of SST in the Niño3.4 box should fall sharply in the coming months, back under 1 ° C in the spring.

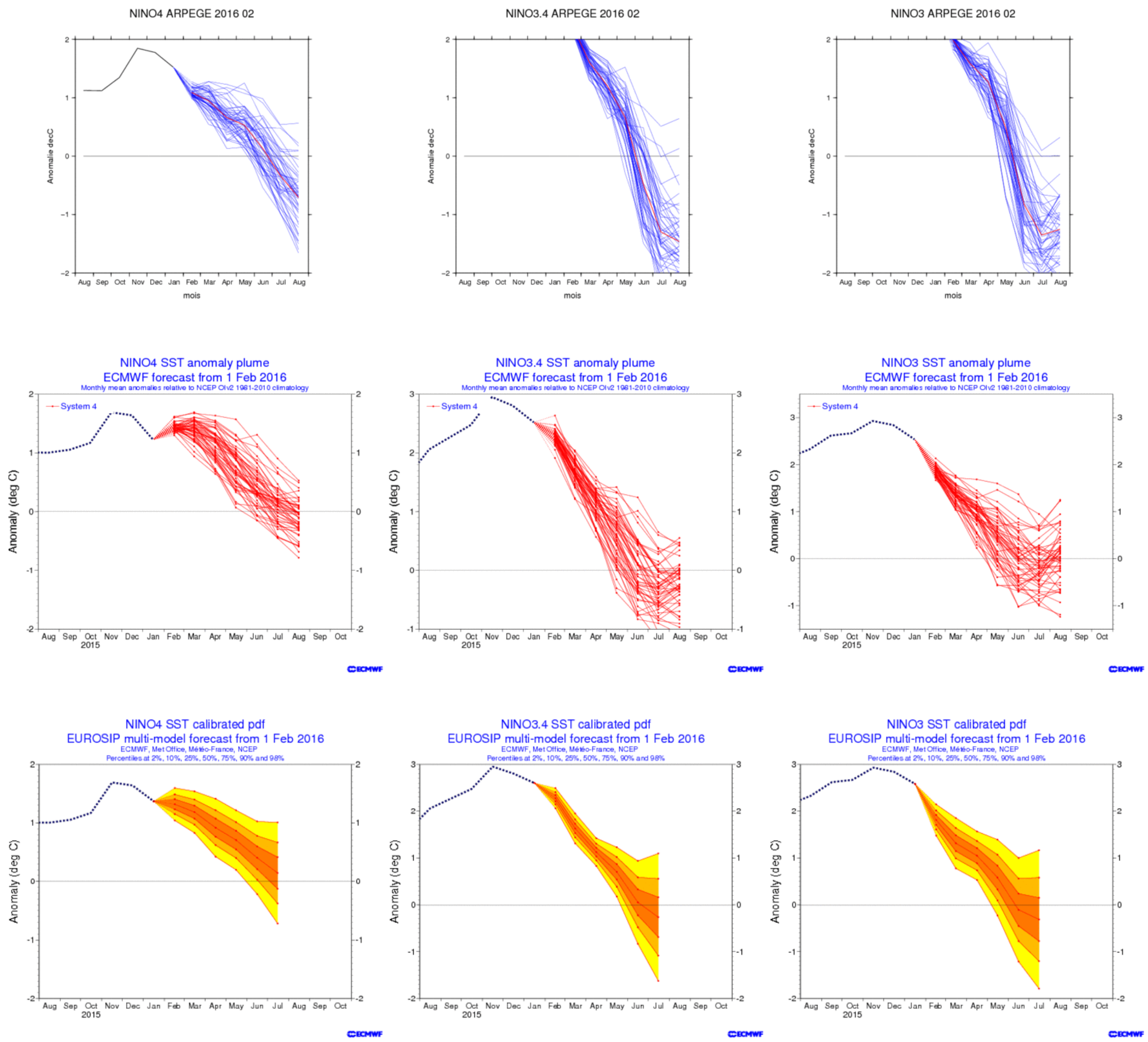

fig.II.1.5: SST anomaly forecasts in the Niño boxes from Météo-France (top) and ECMWF (middle) - monthly mean for individual members - and EuroSIP (bottom) – recalibrated distributions - (http://elaboration.seasonal.meteo.fr , http://www.ecmwf.int/)

II.1.c Atlantic ocean forecasts

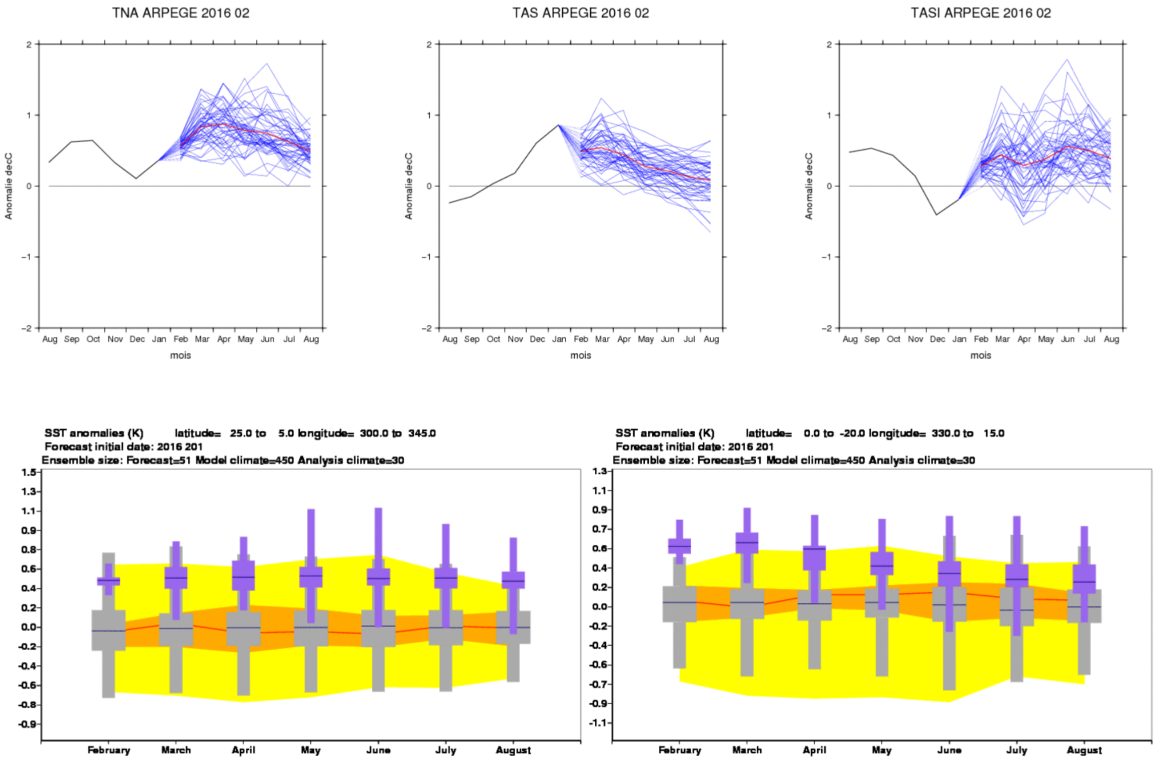

fig.II.1.6: SSTs anomaly forecasts in the Atlantic Ocean boxes from Météo-France and ECMWF, plumes / climagrams correspond to ensemble members and monthly means.

II.1.d Indian ocean forecasts

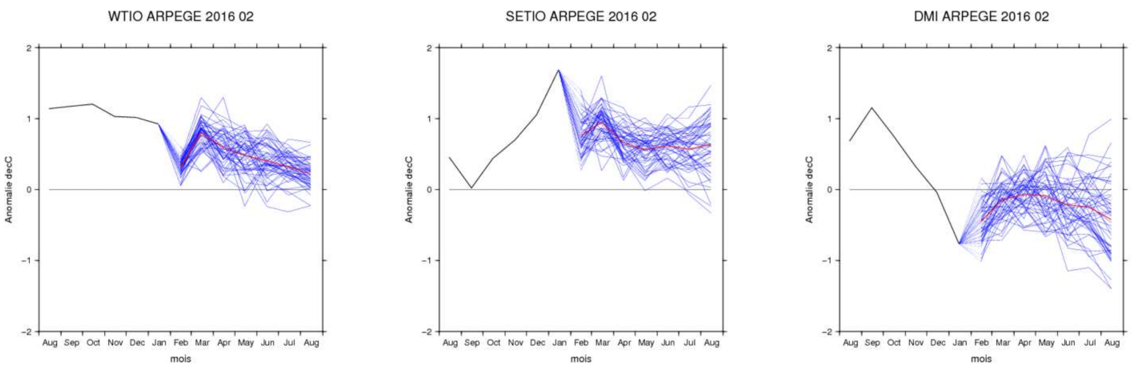

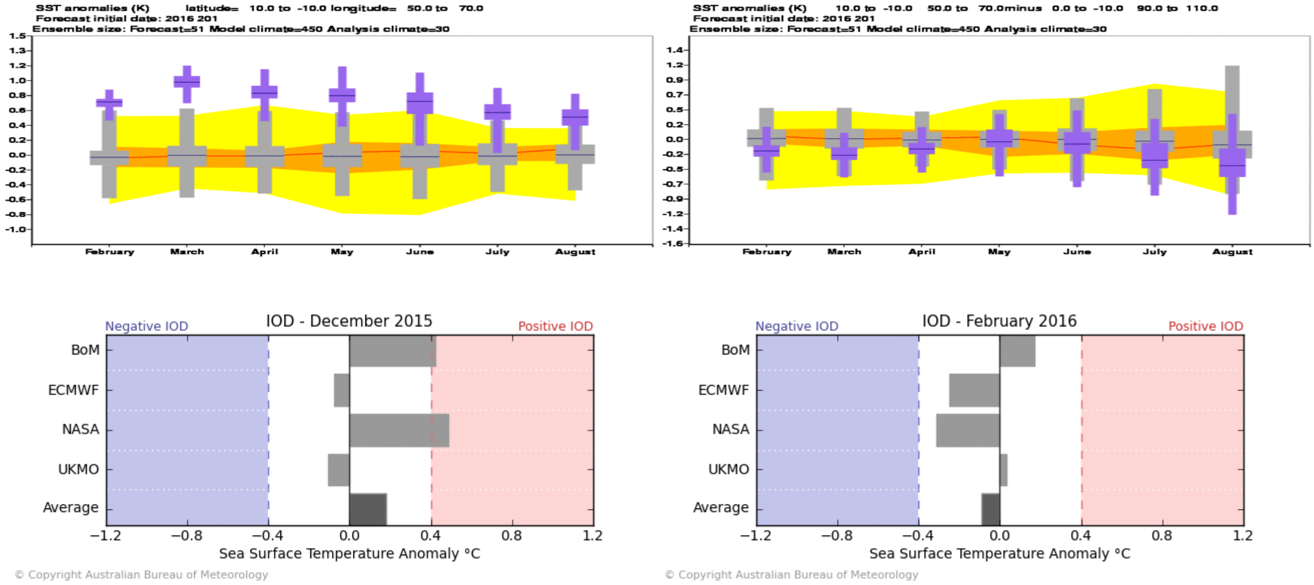

fig.II.1.7: SSTs anomaly forecasts in the Indian Ocean boxes from Météo-France and ECMWF, plumes / climagrams correspond to ensemble members and monthly means.

II.2. GENERAL CIRCULATION FORECAST

II.2.a Global forecast

Velocity potential anomaly field (cf. fig. II.2.1 – insight into Hadley-Walker circulation anomalies) and **Stream Function anomaly field** (cf. fig. II.2.1 – insight into teleconnection patterns tropically forced):

On the Pacific: The models are in good agreement, they plan an upward motion anomaly area in the central and eastern Pacific with an extension to the United States to the north and Chile and Argentina to the south, and very strong anomaly of subsidence on the Maritime Continent extending northward over eastern Asia and the western Pacific. This dipole is stronger in ARP forecast than in the ECMWF one. All the models develop a very structured PNA teleconnection.

In the Atlantic: The 3 models have the same general structure of the fields, but differences are significant. ECMWF offers low velocity potential anomalies with a rather subsiding area on the tropical Atlantic, and a field of highly structured stream function with clear teleconnection towards the middle latitudes and an anticyclonic circulation anomaly over Western Europe. ARPEGE provides a fairly uniform upward motion area with a stream function field much less organized, favoring a cyclonic anomaly over a large part of Northern Europe.

JMA model is close to ECMWF.

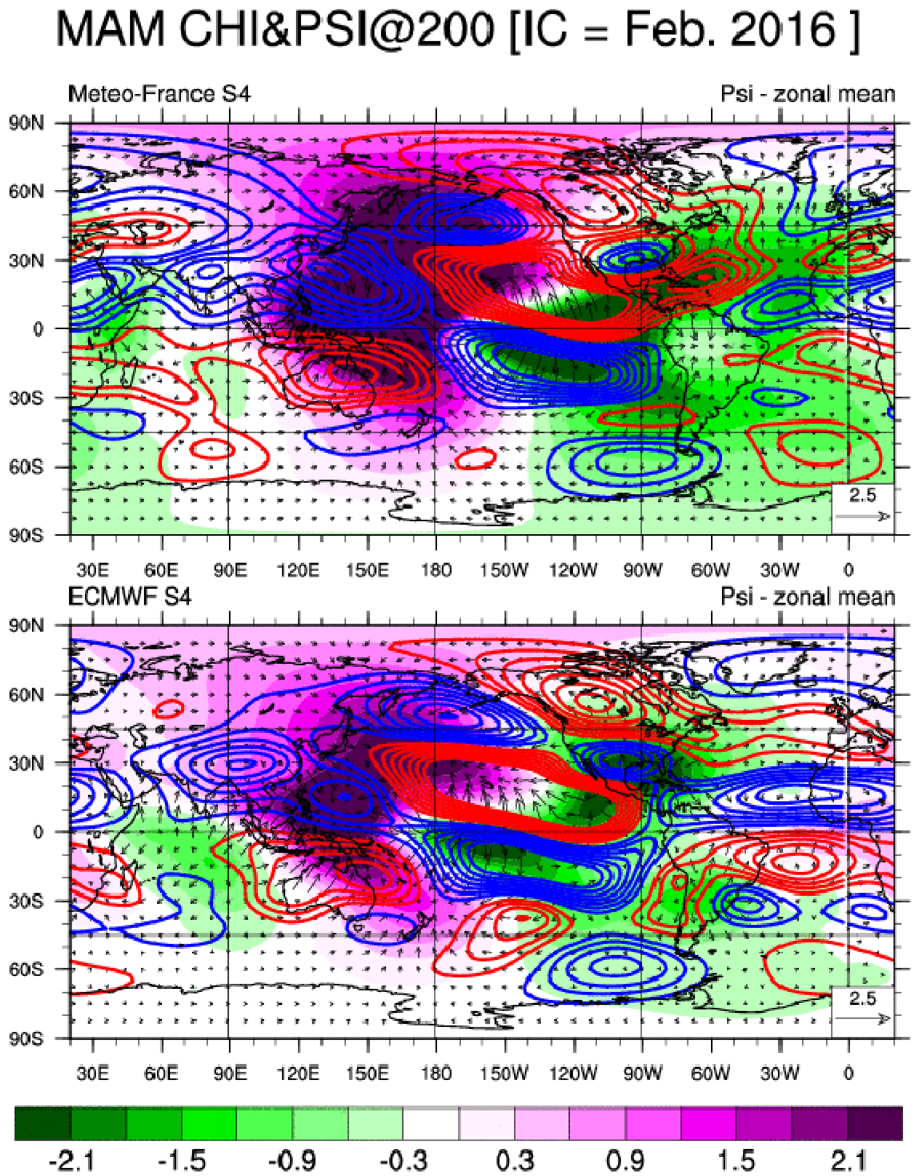

fig.II.2.1: Velocity Potential anomaly field χ (shaded area – green negative anomaly and pink positive anomaly), associated Divergent Circulation anomaly (arrows) and Stream Function anomaly ψ (isolines – red positive and blue negative) at 200 hPa by Météo-France (top) and ECMWF (bottom).

II.2.b North hemisphere forecast and Europe

Geopotential height anomalies (fig. II.2.2 – insight into mid-latitude general circulation anomalies):

Models are consistent on Pacific area with a similar PNA structure. At variance, on the Atlantic and Europe, they diverge clearly. The weather regime forecast is thuso totally opposed. ECMWF seems more coherent and more in the continuity of previous forecasts. On another side, the new ARPEGE system 5 offers a forecast close enough to ECMWF. So we will give preference to the NAO+ option.

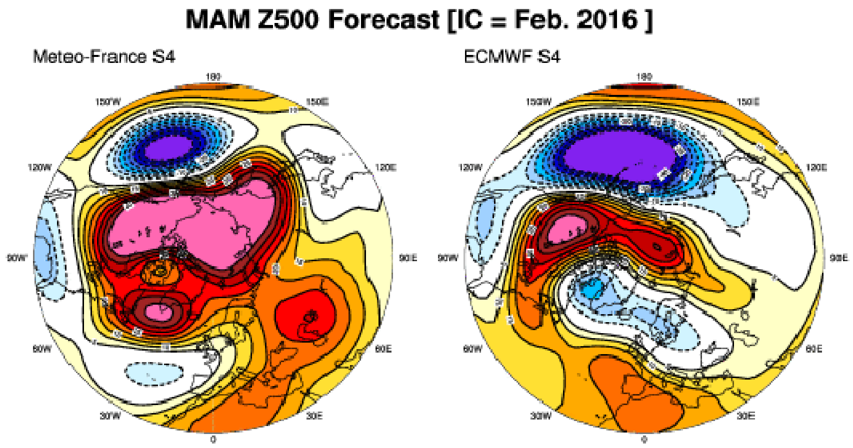

fig.II.2.2: Anomalies of Geopotential Height at 500 hPa from Météo-France (left) and ECMWF (right).

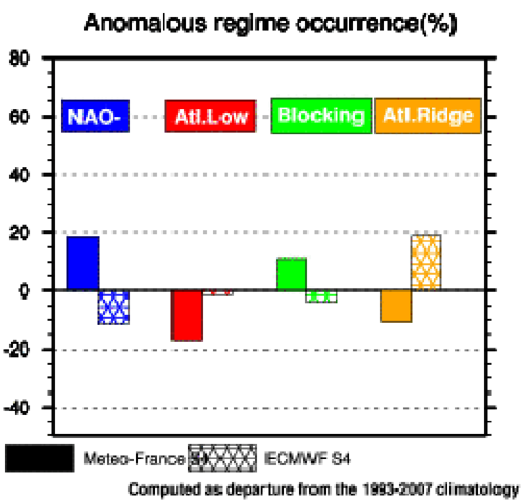

fig.II.2.3: North Atlantic Regime occurrence anomalies from Météo-France and ECMWF : vertical bars represent the excitation frequency anomaly (in %) for each of the 4 regimes.

II.3. IMPACT: TEMPERATURE FORECASTS

In a global context favorable to warm anomalies over most of the globe, there is few exceptions where hot is unlikely. They relate to ocean areas where surface temperatures are expected below normal, and some exceptions on the continents: Mexico and the southern United States, Argentina, southwest of Australia.

On Europe, a "warmer than normal" signal is most likely. The signal, however, is weaker than the months before both probability and intensity.

II.3.a ECMWF

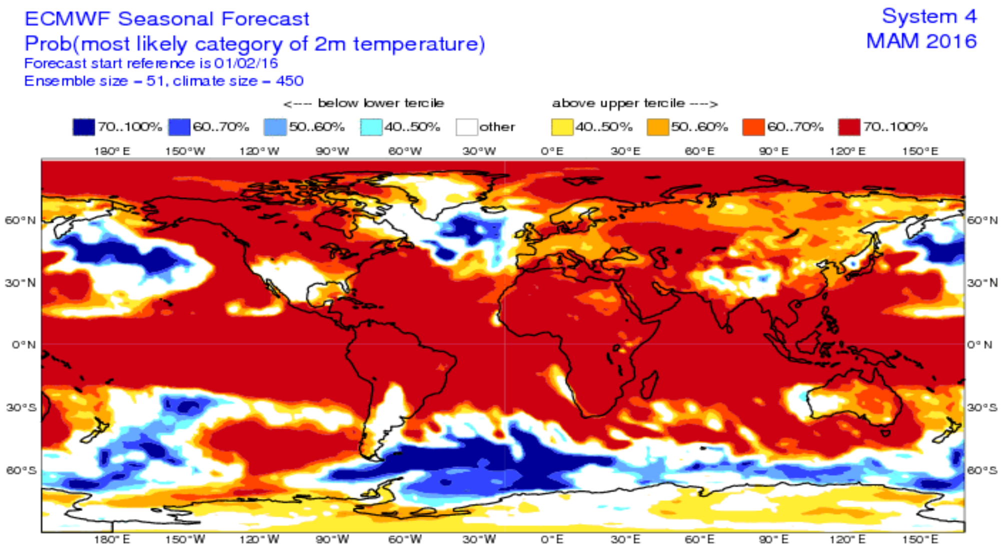

fig.II.3.1: Most likely category probability of T2m from ECMWF. Categories are Above Normal, Below Normal and « other » category (Normal and No Signal). http://www.ecmwf.int/products/forecasts/d/charts/seasonal/forecast/

II.3.b Météo-France

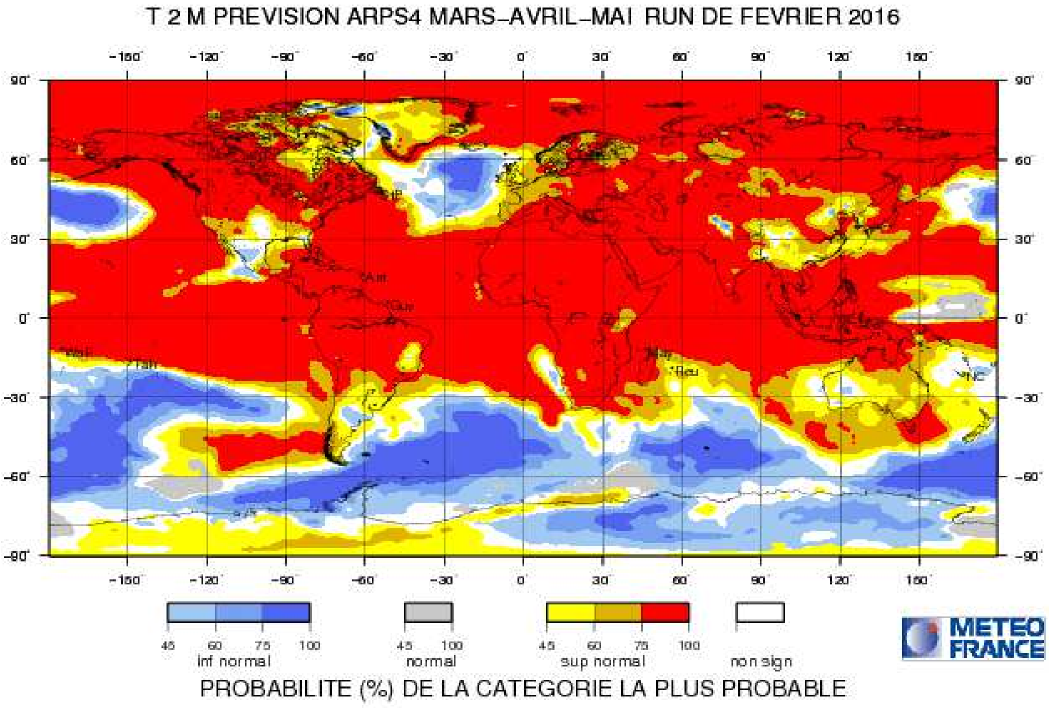

fig.II.3.2: Most likely category of T2m. Categories are Above, Below and Close to Normal. White zones correspond to No Signal. http://elaboration.seasonal.meteo.fr/

II.3.c Japan Meteorological Agency (JMA)

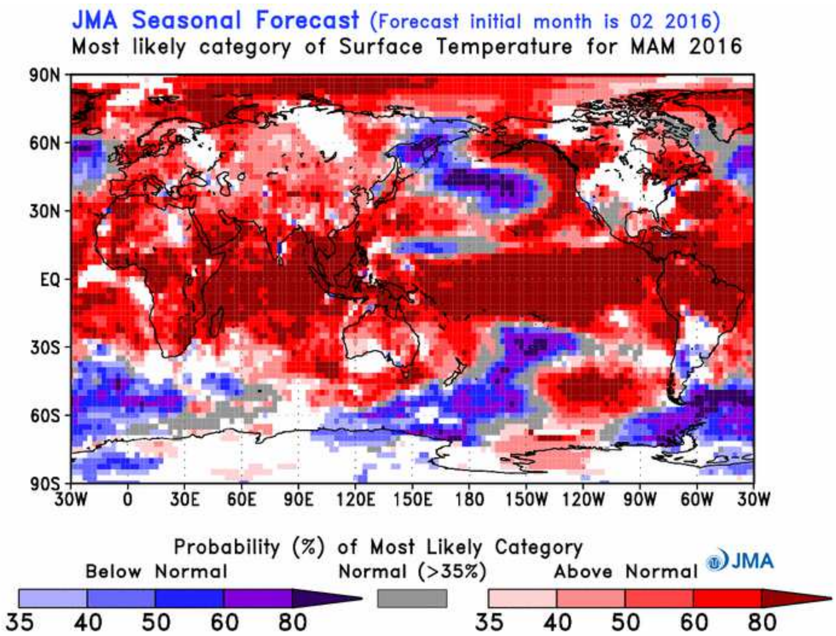

fig.II.3.3: Most likely category of T2m. Categories are Above, Below and Close to Normal. White zones correspond to No Signal. http://ds.data.jma.go.jp/tcc/tcc/products/model/probfcst/4mE/fcst/fcst_gl.php

II.3.d EUROSIP

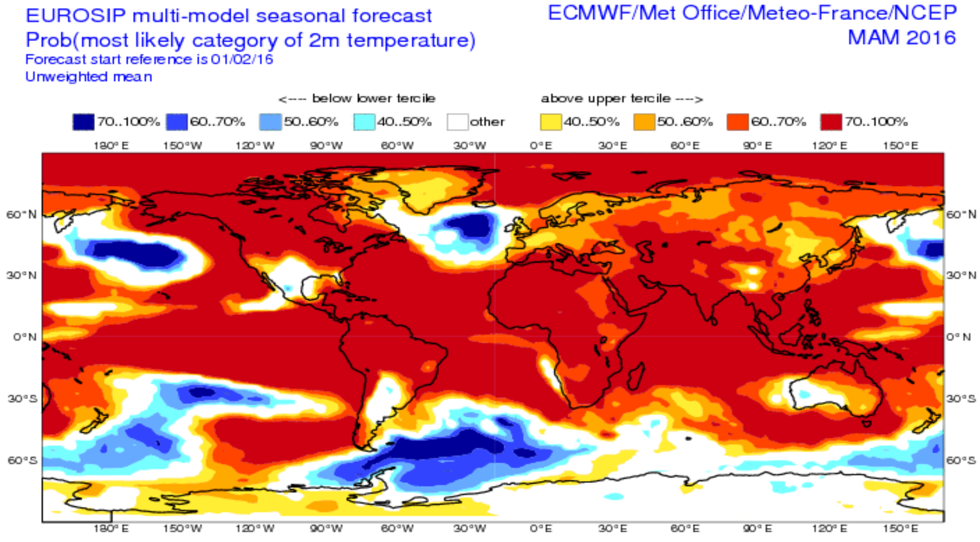

fig.II.3.4: Multi-Model Probabilistic forecasts for T2m from EUROSIP (2 Categories, Below and Above normal – White zones correspond to No signal and Normal).

http://www.ecmwf.int/products/forecasts/d/charts/seasonal/forecast/eurosip/

II.4. IMPACT : PRECIPITATION FORECAST

There is a large contribution of the El Nino event to the forecasted anomalies distribution. Enhanced probability of excess precipitation in central and eastern equatorial Pacific extending North-Eastward to Mexico Gulf and South of USA and Bermudas; and extending south-Eastward to southern South-America. It is surrounded by areas of high probability of lower than normal rainfall over the northeast of Brazil, from Indochinese Peninsula to Hawaii, and from New Guinea south of Polynesia. Excess rainfall is likely over the Indian Ocean, from the Horn of Africa to Indonesia. While Southern Africa should rather be in deficit rainfall.

For Europe, the north-south gradient is expected to remain with dry area on North Africa and the Mediterranean coasts, and increased probability of precipitation above normal further north. The boundary between these two zones is unclear and varies from one model to another.

II.4.a ECMWF

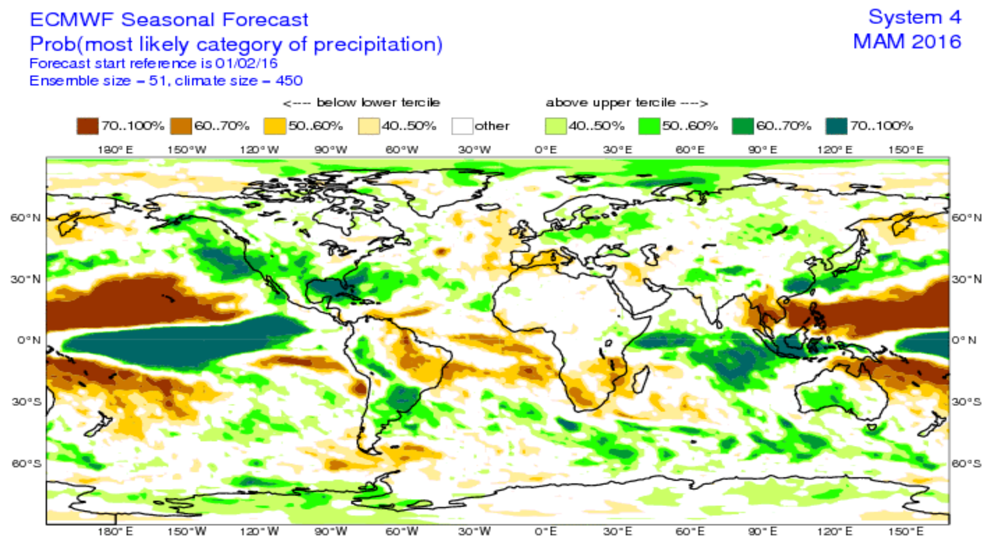

fig.II.4.1: Most likely category probability of rainfall from ECMWF. Categories are Above Normal, Below Normal and « other » category (Normal and No Signal). http://www.ecmwf.int/products/forecasts/d/charts/seasonal/forecast/

II.4.b Météo-France

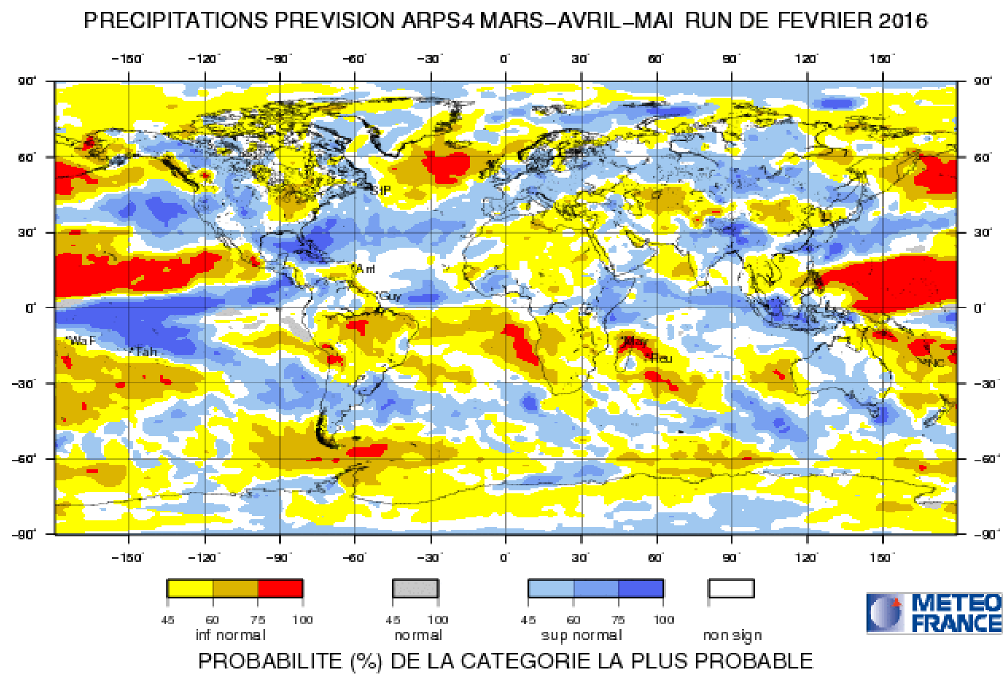

fig.II.4.2: Most likely category of Rainfall. Categories are Above, Below and Close to Normal. White zones correspond to No Signal. http://elaboration.seasonal.meteo.fr/

II.4.c Japan Meteorological Agency (JMA)

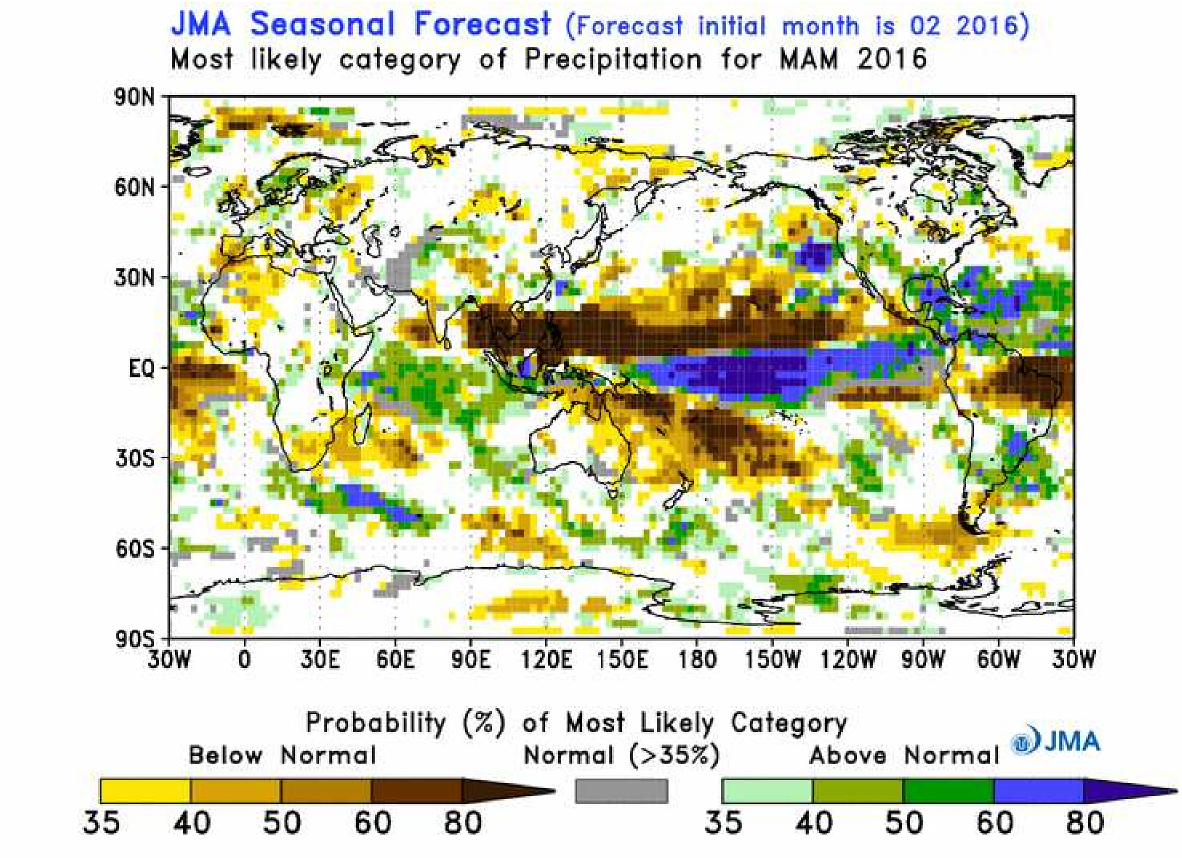

fig.II.4.5: Most likely category of Rainfall from JMA. Categories are Above, Below and Close to Normal. White zones correspond to No Signal. http://ds.data.jma.go.jp/tcc/tcc/products/model/probfcst/4mE/fcst/fcst_gl.php

II.4.d EUROSIP

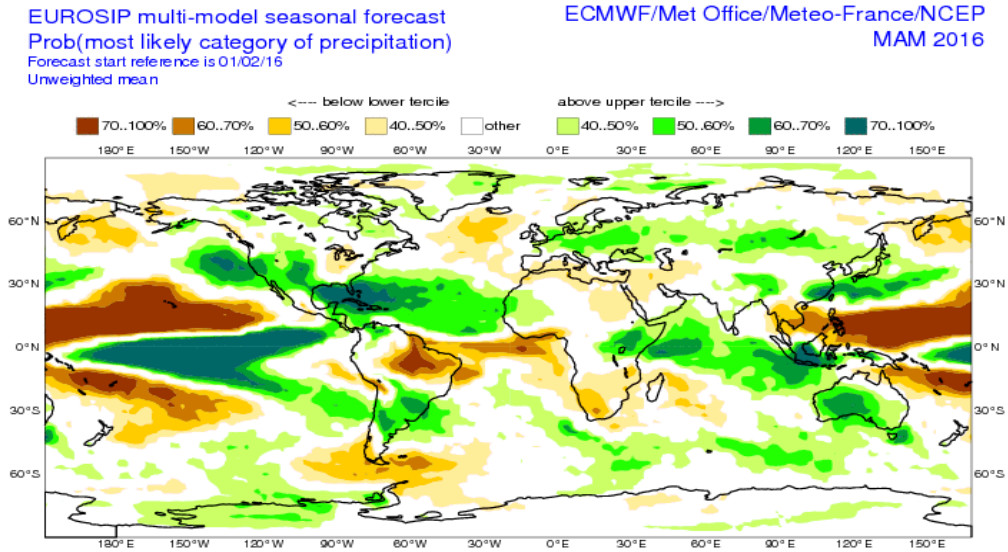

fig.II.4.7: Multi-Model Probabilistic forecasts for precipitation from EUROSIP (2 Categories, Below and Above normal – White zones correspond to No signal).

http://www.ecmwf.int/products/forecasts/d/charts/seasonal/forecast/eurosip/

II.5. REGIONAL TEMPERATURES and PRECIPITATIONS

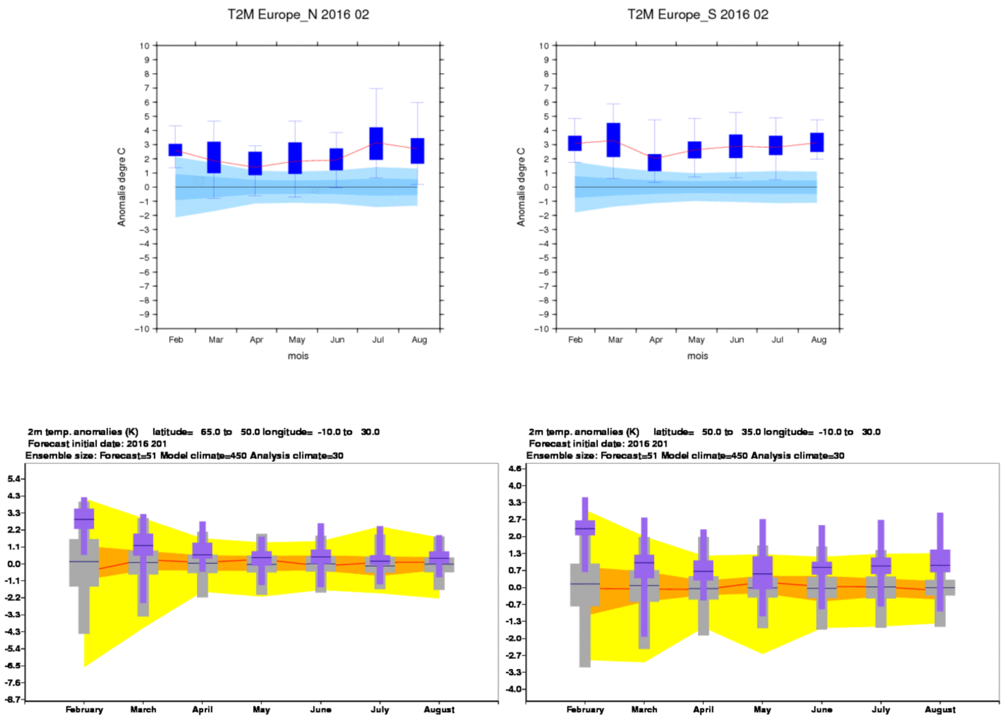

fig.II.5.1 : Climagrams for Temperature in Northern Europe (left) and in Southern Europe (right) from Météo-France (top) and ECMWF (bottom).

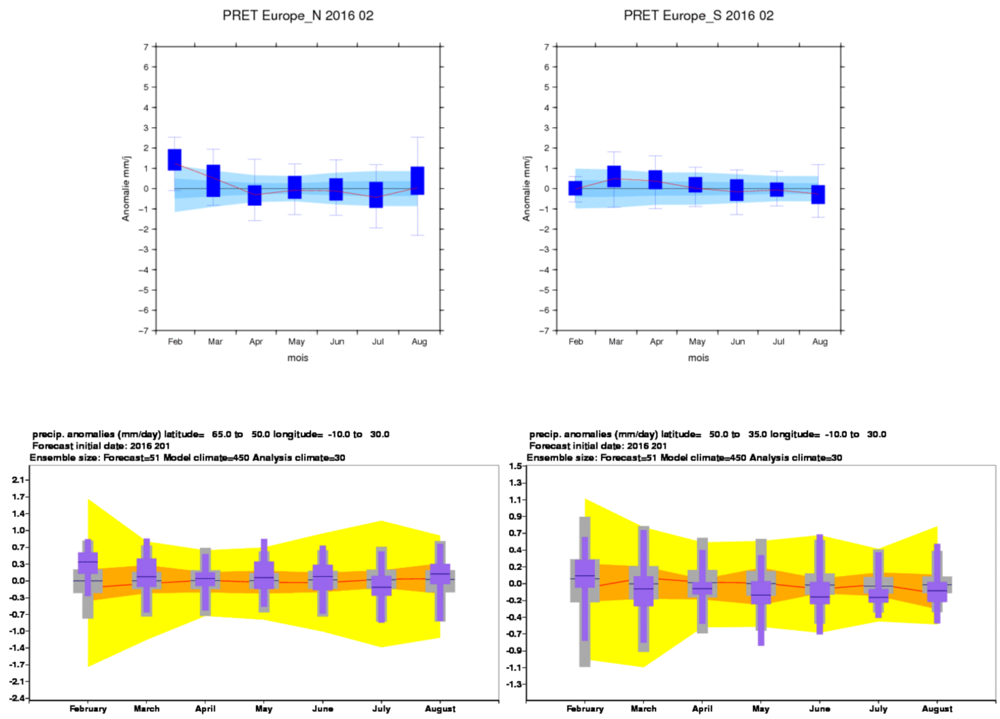

fig.II.5.2 : Climagrams for Rainfall in Northern Europe (left) and in Southern Europe (right) from Météo-France (top) and ECMWF (bottom).

II.6. MODEL'S CONSISTENCY

Not available

fig.II.6.1 : GPCs Consistency maps from LC-MME http://www.wmolc.org/

For SST :

For Z500 :

For T2m :

For Precipitation :

II.7. "EXTREME" SCENARIOS

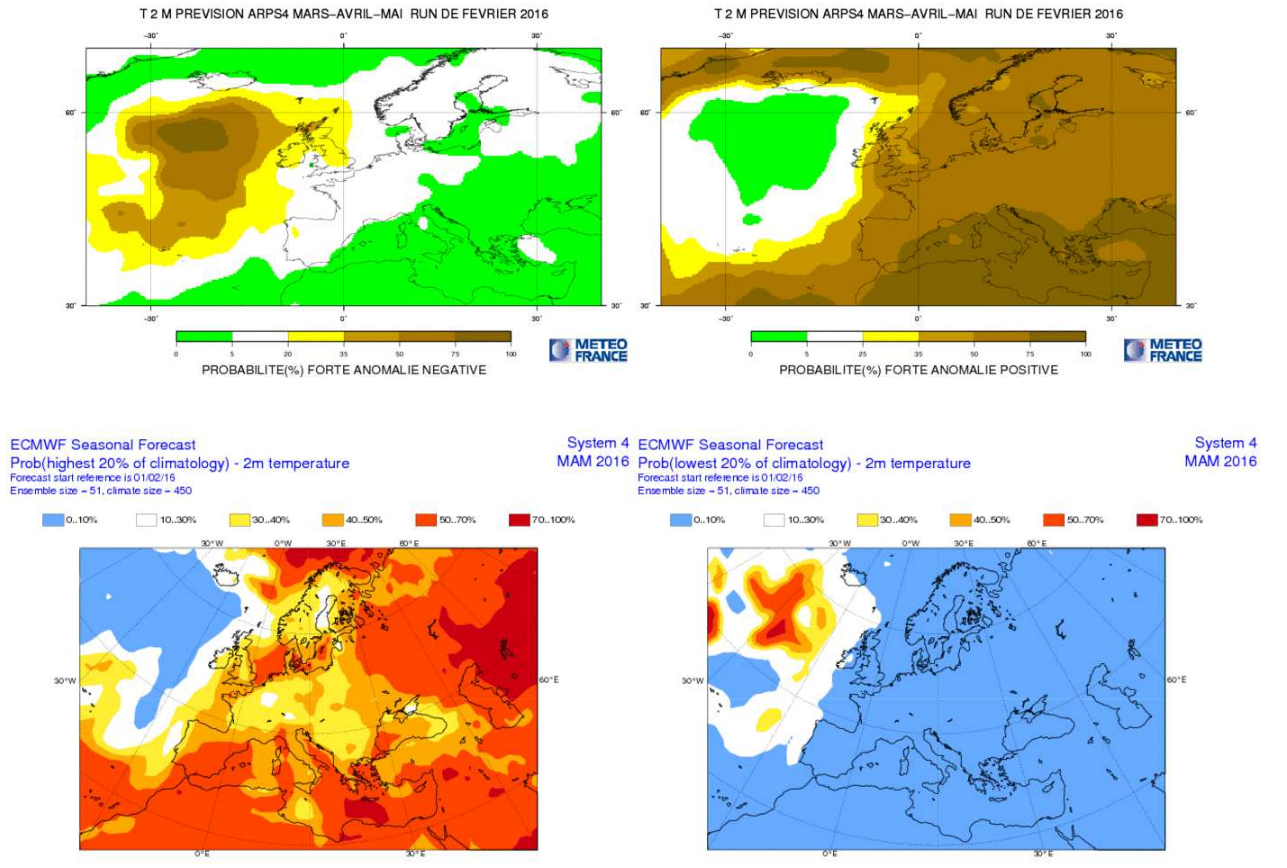

fig.II.7.1 : Top : Meteo-France T2m probability of « extreme » below normal conditions (left - lowest ~15% of the distribution) and "extreme" above normal conditions (right - highest ~15% of the distribution). Bottom : ECMWF T2m probability of « extreme » below normal conditions (left - lowest ~20% of the distribution) and "extreme" above normal conditions (right – highest ~20% of the distribution).

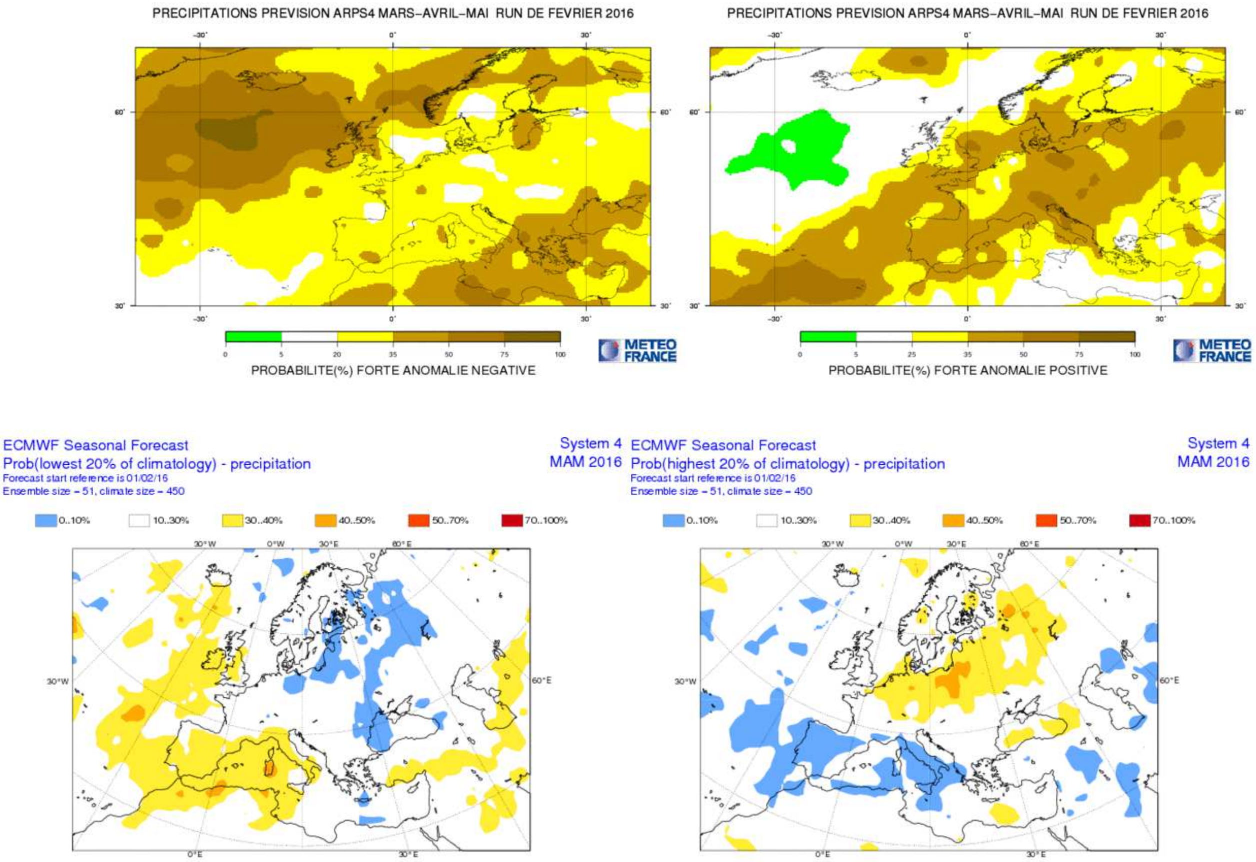

fig.II.7.2 : Top : Meteo-France rainfall probability of « extreme » below normal conditions (left - lowest ~15% of the distribution) and "extreme" above normal conditions (right - highest ~15% of the distribution).
Bottom : ECMWF rainfall probability of « extreme » below normal conditions (left - lowest ~20% of the distribution) and "extreme" above normal conditions (right – highest ~20% of the distribution).

II.8. DISCUSSION AND SUMMARY

II.8.a Forecast over Europe

Temperatures: warm anomaly is likely.

Precipitation: dry anomaly is very likely on southern Europe and around the Mediterranean Sea.
Likely wet anomaly on Continental Europe and no scenario elsewhere.

Prévisions saisonnières probabilistes de températures pour le trimestre prochain

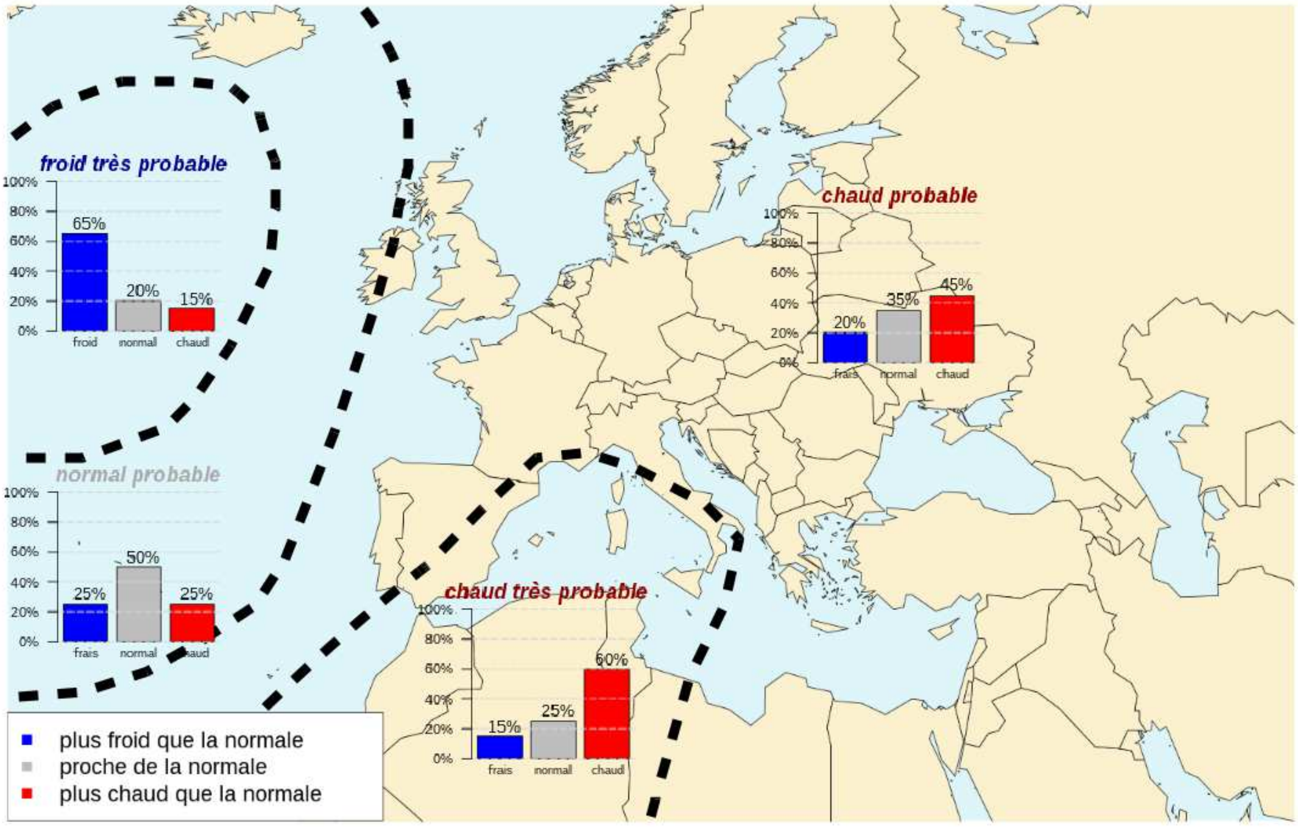

Mars-Avril-Mai 2016

Prévisions saisonnières probabilistes de précipitations pour le trimestre prochain

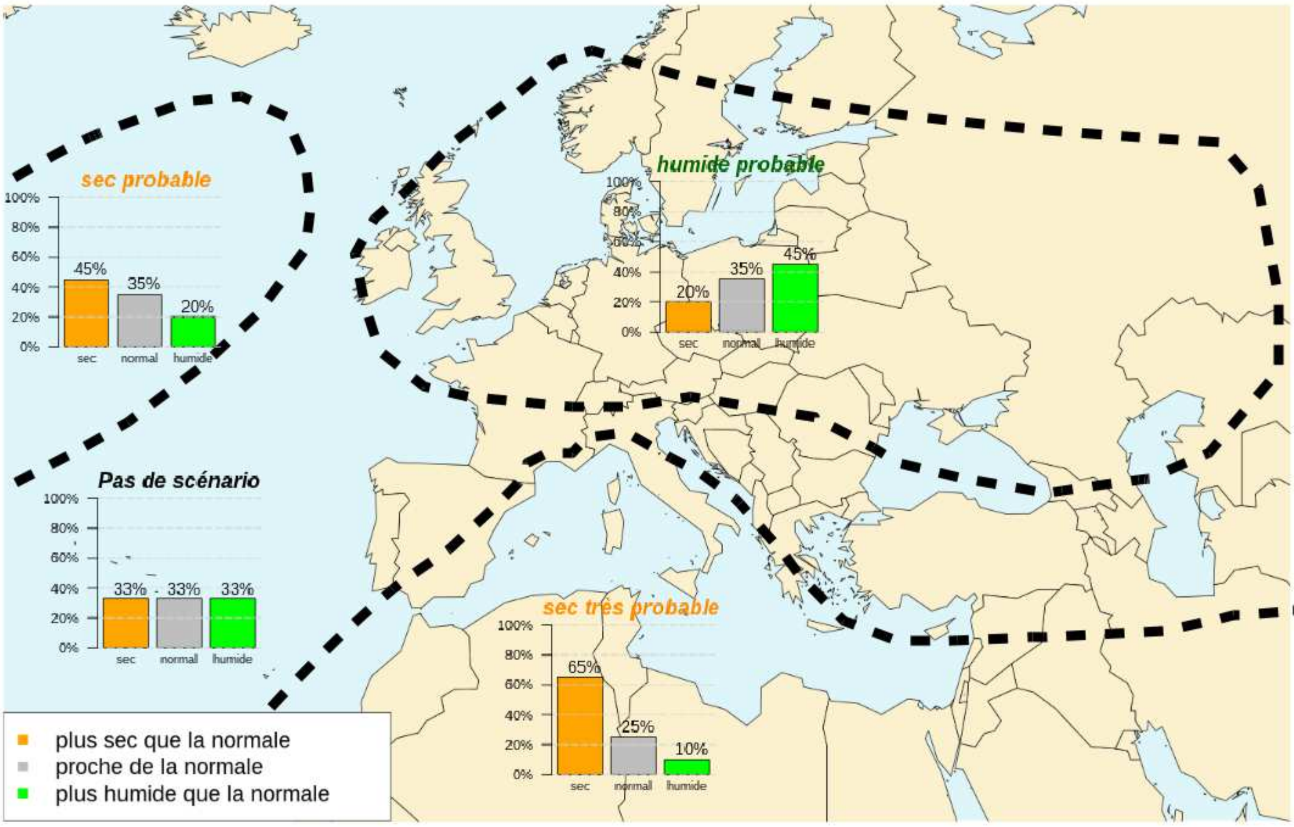

Mars-Avril-Mai 2016

II.8.b Tropical cyclone activity

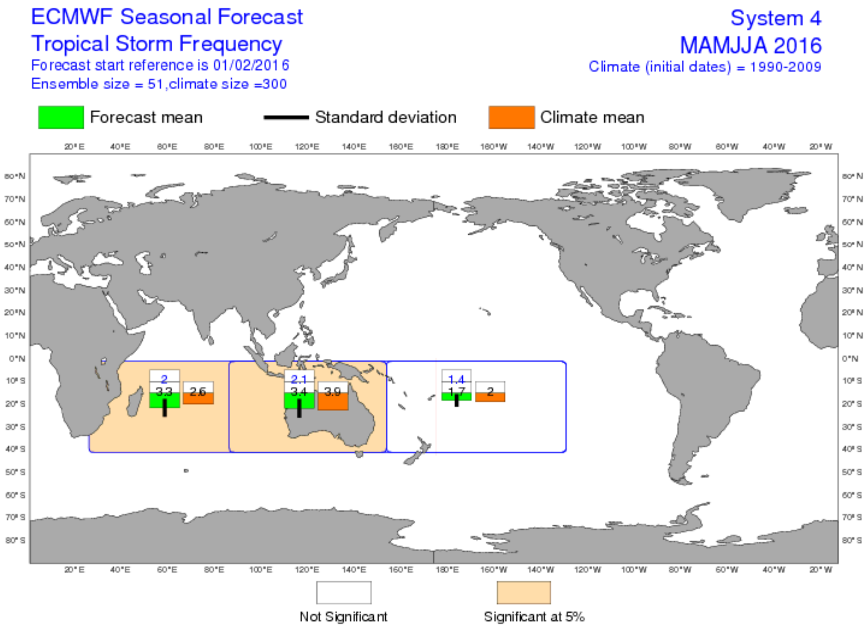

fig.II.8.1: Seasonal forecast of the frequency of Tropical Cyclones from EUROSIP (Météo-France & ECMWF).
http://www.ecmwf.int/products/forecasts/d/charts/seasonal/forecast/eurosip/

The end of hurricane season is expected stronger than normal over Indian Ocean.

ANNEX

II.9. SEASONAL FORECASTS

Presently several centres provide seasonal forecasts, especially those designated as Global Producing Centres by WMO (see http://www.wmo.int/pages/prog/wcp/wcasp/clips/producers_forecasts.html).

■ BoM, CMA, CPTEC, ECMWF, JMA, KMA, Météo-France, NCEP and UK Met Office have ocean/atmosphere coupled models. The other centres have atmospheric models which are forced by a SST evolution which is prescribed for the entire period of forecast.

■ LC-MME and Euro-SIP provide multi-model forecasts. Euro-Sip is presently composed using 4 models (ECMWF, Météo-France, NCEP and UK Met Office). LC-MME uses information coming from most of the GPCs ; providing deterministic and probabilistic combinations of several coupled and forced models.

Seasonal forecasts use the ensemble technique to sample uncertainty sources inherent to these forecasts. Several Atmospheric and/or oceanic initial states are used to perform several forecasts with slightly different initial state in order to sample the uncertainty related to imperfect knowledge of the initial state of the climate system. When possible, the model uncertainty is sampled using several models or several version of the same model. The horizontal resolution of the Global models is currently between 100 and 300km. This mean that only Large Scale feature make sense in the interpretation of the issued forecasts. Generally speaking, the temperature forecasts show better skills than rainfall forecasts. Then, it exists a natural weakness of the seasonal predictability in Spring (ref to North Hemisphere).

In order to better interpretate the results, it is recommended to look to verification maps and graphs which give some insight into the expected level of skill for a specific parameter, region and period. A set of scores is presented on the web-site of the Lead-Centre for Verification (see http://www.bom.gov.au/wmo/lrfvs/) ; scores are also available at the specific web site of each centres.

This bulletin collects all the information available the 21st of the current month preceding the forecasted 3-month period.

II.10. « NINO », SOI INDICES AND OCEANIC BOXES

El Niño and La Niña events primarily affect tropical regions and are monitored by following the SST evolution in specific area of the equatorial Pacific.

- Niño 1+2 : 0°/10°S 80W-90W ; it is the region where the SST warming is developing first at the surface (especially for coastal events).
- Niño 3 : 5°S/5°N 90W-150W ; it is the region where the interanual variability of SST is the greatest.
- Niño 4 : 5°S/5°N 160E- 150 W ; it is the region where SST evolution have the strongest relationship with evolution of convection over the equatorial Pacific.
- Niño 3.4 : 5°S/5°N 120W-170W ; it is a compromise between Niño 3 and Niño 4 boxes (SST variability and Rainfall impact).

Associated to the oceanic « El Niño / La Niña » events, and taking into account the strong ocean/atmopshere coupling, the atmosphere shows also interanual variability associated to these events. It is monitored using the SOI (Southern Oscillation Index). This indice is calculated using standardized sea level pressure at Tahiti minus standardized sea level pressure at Darwin (see above figure). It represents the Walker (zonal) circulation and its modifications. Its sign is opposite to the SST anomaly meaning that when the SST is warmer (respectively colder) than normal (Niño respectively Niña event), the zonal circulation is weakened (respectively strengthened).

Oceanic boxes used in this bulletin :

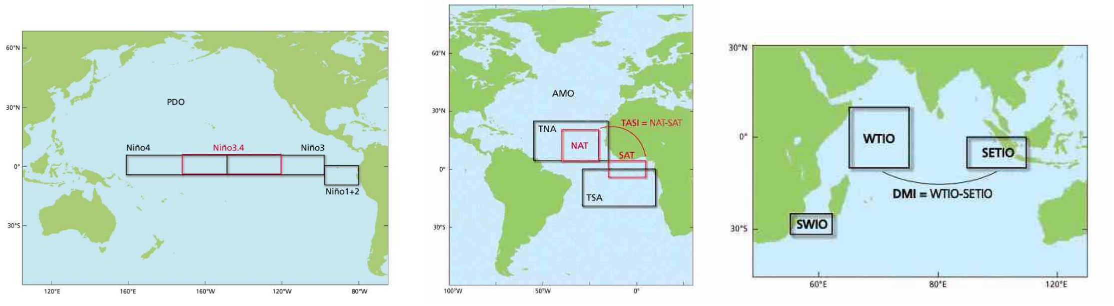

II.11.LAND BOXES

Some forecasts correspond to box averaged values for some specific area over continental regions. These boxes are described in the following map and are common to ECMWF and Météo-France.

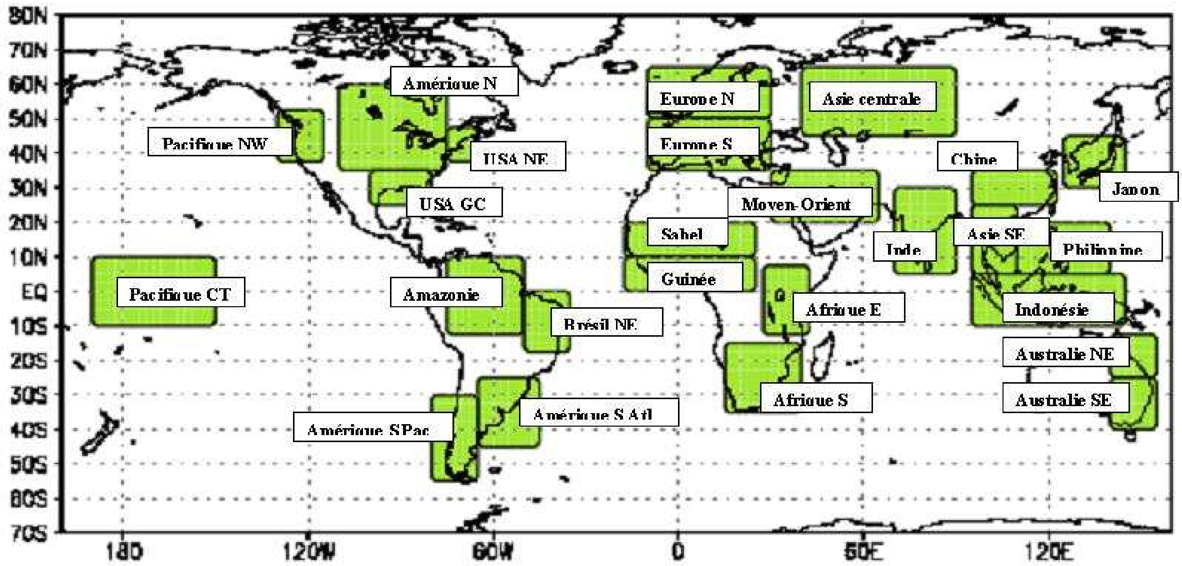

II.12. ACKNOWLEDGEMENT

This bulletin is edited by the RCC-LRF Node of the RCC Network in Toulouse for the RA VI. It is a joint effort of the RCC-Climate Monitoring Node (led by DWD) and the RCC-LRF Node (Co-Led by Météo-France).